iScience

CellPress
OPEN ACCESS

Article

Caveolin-1 peptide regulates p53-microRNA-34a feedback in fibrotic lung fibroblasts

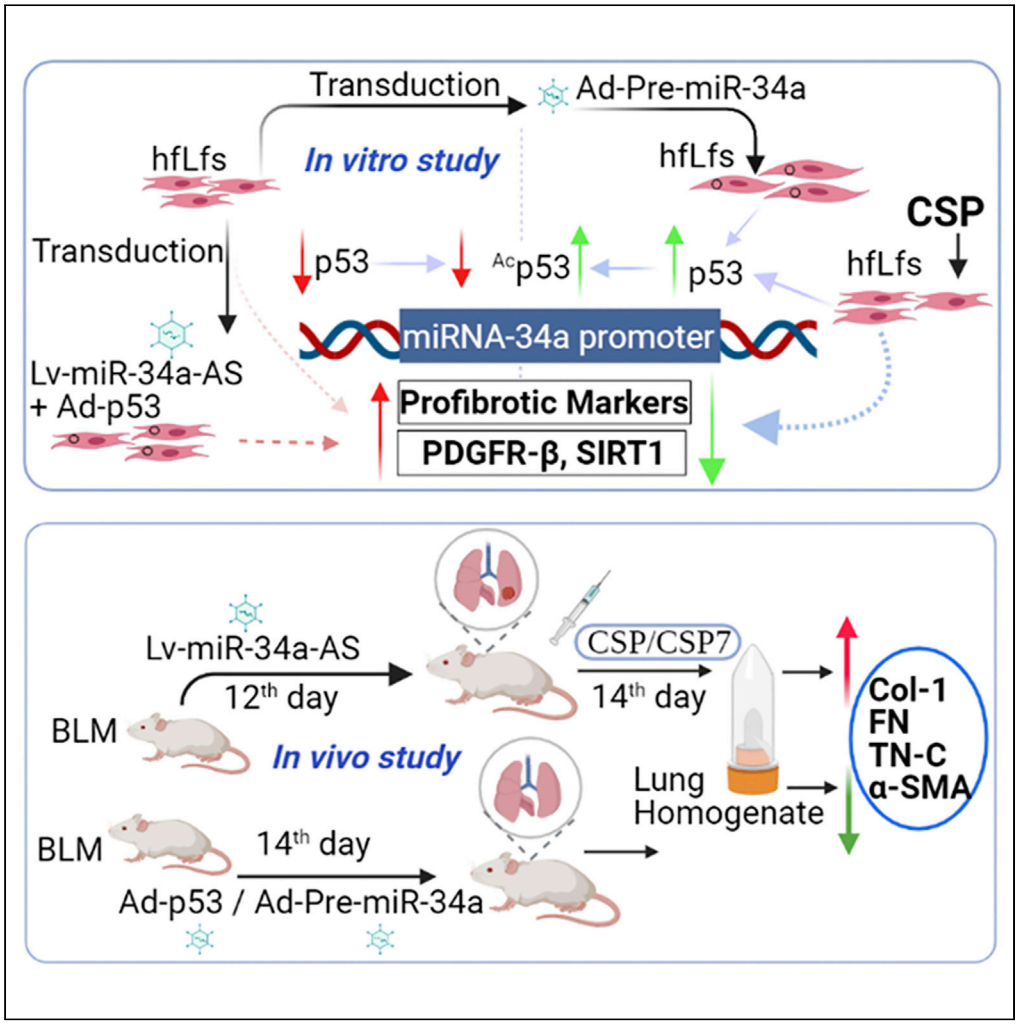

Taryn B. Hogan, Nivedita Tiwari, M.R. Nagaraja, ..., Rashmi S. Shetty, Yashodhar P. Bhandary, Sreerama Shetty

sreerama.shetty@uthct.edu

Highlights

FLfs showed decreased basal miR-34a levels and reduced binding of p53

CSP/CSP7-mediated dedifferentiation of fLfs required miR-34a expression

Mice lacking miR-34a in fibroblasts are susceptible to PF and resist CSP/CSP7

Hogan et al., iScience 25, 104022
April 15, 2022
https://doi.org/10.1016/j.isci.2022.104022

iScience

CellPress
OPEN ACCESS

Article

Caveolin-1 peptide regulates p53-microRNA-34a feedback in fibrotic lung fibroblasts

Taryn B. Hogan,[1,3] Nivedita Tiwari,[1,3] M.R. Nagaraja,[1,3] Shwetha K. Shetty,[1,2] Liang Fan,[1] Rashmi S. Shetty,[1] Yashodhar P. Bhandary,[1] and Sreerama Shetty[1,4,*]

SUMMARY

Idiopathic pulmonary fibrosis (IPF) is a life-threatening disease resulting from dysregulated repair responses to lung injury. Excessive extracellular matrix deposition by expanding myofibroblasts and fibrotic lung fibroblasts (fLfs) has been implicated in the pathogenesis of PF, including IPF. We explored fLfs' microRNA-34a (miR-34a) expression from IPF tissues. Basal miR-34a levels were decreased with reduced binding of p53 to the promoter DNA and 3′UTR mRNA sequences. Overexpression of miR-34a in fLfs increased p53, PAI-1, and reduced pro-fibrogenic markers. The regulatory effects of miR-34a were altered by modifying the p53 expression. Precursor-miR-34a lung transduction reduced bleomycin-induced PF in wild-type mice. fLfs treated with caveolin-1 scaffolding domain peptide (CSP) or its fragment, CSP7, restored miR-34a, p53, and PAI-1. CSP/CSP7 reduced PDGFR-β and pro-fibrogenic markers, which was abolished in fLfs following blockade of miR-34a expression. These peptides failed to resolve PF in mice lacking miR-34a in fLfs, indicating miR-34a-p53-feedback induction required for anti-fibrotic effects.

INTRODUCTION

Pulmonary fibrosis (PF) is a heterogeneous group of interstitial lung diseases (ILDs) associated with substantial morbidity and mortality (Olson et al., 2007). These disorders are characterized by alveolar progenitor type II epithelial cell (AEC) senescence and apoptosis, and accumulation of activated myofibroblasts and fibrotic lung fibroblasts (fLfs). fLfs have a higher rate of proliferation and resist apoptosis. They have increased migration and invasiveness, and more readily deposit extracellular matrix (ECM) than lung fibroblasts (Lfs) from histologically "normal" lungs (nLfs) (King et al., 2011; Noble and Homer, 2004; Phan, 2002; Suganuma et al., 1995). This leads to progressive destruction of alveolar architecture and loss of lung function. IPF is the most common and fatal form of ILDs with an estimated incidence of 40–50 cases per 100,000 individuals in the United States (Esposito et al., 2015). Most patients present with advanced disease at diagnosis, which accounts for the bleak prognosis with a median 5-year survival of only 20% (Gomer and Lupher, 2010). Until recently, IPF has been refractory to all pharmacologic interventions. Lung transplantation is the only viable option for patients with end-stage PF but is only available to a minority of patients. In 2014, two small-molecule drugs pirfenidone and nintedanib were approved by the FDA for the treatment of IPF. These drugs slow the decline of lung function but are not curative (King et al., 2014; Richeldi et al., 2014).

MicroRNA-34a (miR-34a) is a transcriptional target of the tumor suppressor protein, p53, and plays a pivotal role in stabilization of p53 by blocking histone deacetylase (HDAC), sirtuin-1 (Sirt1) (Yamakuchi and Lowenstein, 2009). Further, miR-34a suppresses the translation of platelet-derived growth factor receptor-β (PDGFR-β) mRNA by binding to the seed sequences present in the 3′UTR (Garofalo et al., 2013), while p53 inhibits PDGFR-β transcription (Yang et al., 2008). miR-34a also regulates cell-cycle arrest through stabilization of p53 and many other target genes. Loss of 1p36.22 (genomic interval harboring miR-34a) is common in diverse human cancers. miR-34a is markedly induced by p53 (Raver-Shapira et al., 2007) and thus promotes p53-mediated cellular events (Fridman and Lowe, 2003). We recently reported that miR-34a expression is increased in injured AECs, which contributes to reduced viability of AECs because of increased expression of p53 (Shetty et al., 2017). Furthermore, miR-34a expression is lost in Lfs of aged mice with bleomycin (BLM)-induced PF (Cui et al., 2017b).

[1]Texas Lung Injury Institute, Department of Medicine, University of Texas Health Science Center at Tyler, 11937 US Highway 271, Tyler, TX 75708, USA

[2]Biochemistry, University of Iowa Carver College of Medicine, Iowa City, IA 52242, USA

[3]These authors contributed equally

[4]Lead contact

*Correspondence: sreerama.shetty@uthct.edu

https://doi.org/10.1016/j.isci.2022.104022

The caveolins are coat proteins of caveolae, which are invaginations of the plasma membranes. Caveolin-1 (Cav1), a major protein of caveolae, is expressed by AECs, endothelial cells, and Lfs (Rothberg et al., 1992). Cav1 traffics to and from the cell membrane with several organelles and is also a soluble component of the cytoplasm (Fridolfsson et al., 2014). Cav1 is increased in injured AECs, whereas lost in activated fLfs including AECs and fLfs from the lungs of patients with IPF or mice with PF. Increased Cav1 in AECs augments senescence and apoptosis leading to PF, whereas its loss in AECs protects the mice from lung injury and PF (Shivshankar et al., 2012). Loss of Cav1 in Lfs, including fLfs leads to its activation and fibroproliferation (Nagaraja et al., 2018; Tourkina et al., 2008; Wang et al., 2006). We found that the Cav1 scaffolding domain peptide (CSP) or its seven amino acids deletion fragment (FTTFTVT); CSP7 concurrently restores AEC renewal and restrains expansion of fLfs leading to mitigation of PF (Marudamuthu et al., 2019; Nagaraja et al., 2018; Shetty et al., 2017).

In this study, we explored whether low levels of p53 and miR-34a found in fLfs were associated with reduced binding of p53 protein with miR-34a promoter and urokinase plasminogen activator (uPA), uPA receptor (uPAR), and plasminogen activator inhibitor-1 (PAI-1) 3′UTR sequences. We then examined whether inhibition of miR-34a in nLfs augments expression of platelet derived growth factor-β (PDGFR-β) and pro-fibrogenic markers, and increases the rate of proliferation, migration, and invasion. Further, we sought whether the process involves parallel inhibition of p53 acetylation and suppression of PAI-1 in these cells. We also tested whether overexpression of miR-34a in fLfs causes opposite responses, and if inhibition of miR-34a attenuates anti-fibrotic effects of p53 in fLfs. We then tested whether treatment of fLfs with CSP/CSP7 augments miR-34a along with acetylated and total p53, and PAI-1. Furthermore, we checked if the process involves miR-34a-mediated suppression of Sirt1 and PDGFR-β with concurrent increase in the miR-34a promoter binding. We concluded the study by testing anti-fibrogenic effects of CSP/CSP7 in fLfs after suppression of miR-34a, as well as their ability to resolve BLM-induced existing PF in tamoxifen-inducible conditional miR-34a knockout (miR-34a^{cKO}) mice lacking its expression in fibroblasts. Our findings suggest that restoration of the p53-miR-34a feedback by CSP/CSP7 can mitigate pro-fibrogenic properties and resolve existing PF through dedifferentiation of fLfs.

RESULTS

PF is typified by tenacious activation of fLfs. fLfs extracted from IPF lungs manifest sustained contractility, rate of growth, resistance to apoptosis, and increased ECM deposition. We previously demonstrated increased activation of fLfs because of loss of baseline expression of p53 (Nagaraja et al., 2018). This has been attributed to reduced expression of Cav1 by fLfs. Augmentation of Cav1, CSP, or CSP7 in fLfs increases baseline p53 level and inhibits well established pro-fibrogenic markers such as type I collagen (Col1), fibronectin (FN), tenascin-C (TN-C), and alpha-smooth muscle actin (α-SMA) (Nagaraja et al., 2018). In continuing our effort to describe the role of p53 pathway in the pathogenesis of PF and anti-fibrogenic responses of Cav1 or CSP/CSP7, we studied the expression of miR-34a for being a transcriptional target of p53. Moreover, miR-34a induces cellular senescence and apoptosis, and regulates translation of multiple genes involved in cell-cycle regulation.

We initially tested miR-34a levels and confirmed that consistent with reduced p53 expression, quantitative real-time PCR (qRT-PCR) analyses revealed that basal expression of miR-34a was significantly reduced in fLfs compared to their corresponding levels in nLfs (Figure 1A). Next, we analyzed miR-34a promoter activity using a reporter assay. In agreement with loss of miR-34a expression in fLfs, the baseline luciferase activity and luciferase antigen expression were significantly reduced in fLfs (Figure 1B). We next analyzed the nLf and fLf lysates for binding to the p53 promoter consensus sequences by gel mobility shift assay. As shown in Figure 1C, lysates of nLfs formed a specific complex with p53 promoter DNA consensus sequence, which in agreement with the absence of p53 expression in fLfs (Nagaraja et al., 2018), was not formed with the fLf lysates, indicating a lack of p53-mediated transcriptional activation. To further confirm the specificity of p53-promoter DNA binding, reaction mixtures were incubated with 0-fold to 100-fold molar excess of unlabeled promoter consensus sequences. As shown in Figure 1D, incubation of nLf lysates with increasing concentrations of unlabeled promoter consensus DNA sequence-inhibited the formation of specific protein-^{32}P-labeled DNA complex. This suggests the specificity of p53 binding to its promoter sequence. Because p53 also directly binds to uPA, uPAR and PAI-1 3′UTR mRNA *cis* determinants, and regulates their expression at the posttranscriptional level (Bhandary et al., 2013), we incubated nLf and fLf lysates with ^{32}P-labeled chimeric uPA-uPAR-PAI-1 3′UTR mRNA sequences and analyzed the RNase T1-resistant protein-3′UTR mRNA complex by gel mobility shift assay. As shown in Figure 1E, consistent with relatively higher basal p53 expression in nLfs, the nLf lysates formed an RNA-protein complex with ^{32}P-labeled chimeric uPA-uPAR-PAI-1 3′UTR mRNA sequences. The specificity of p53 binding

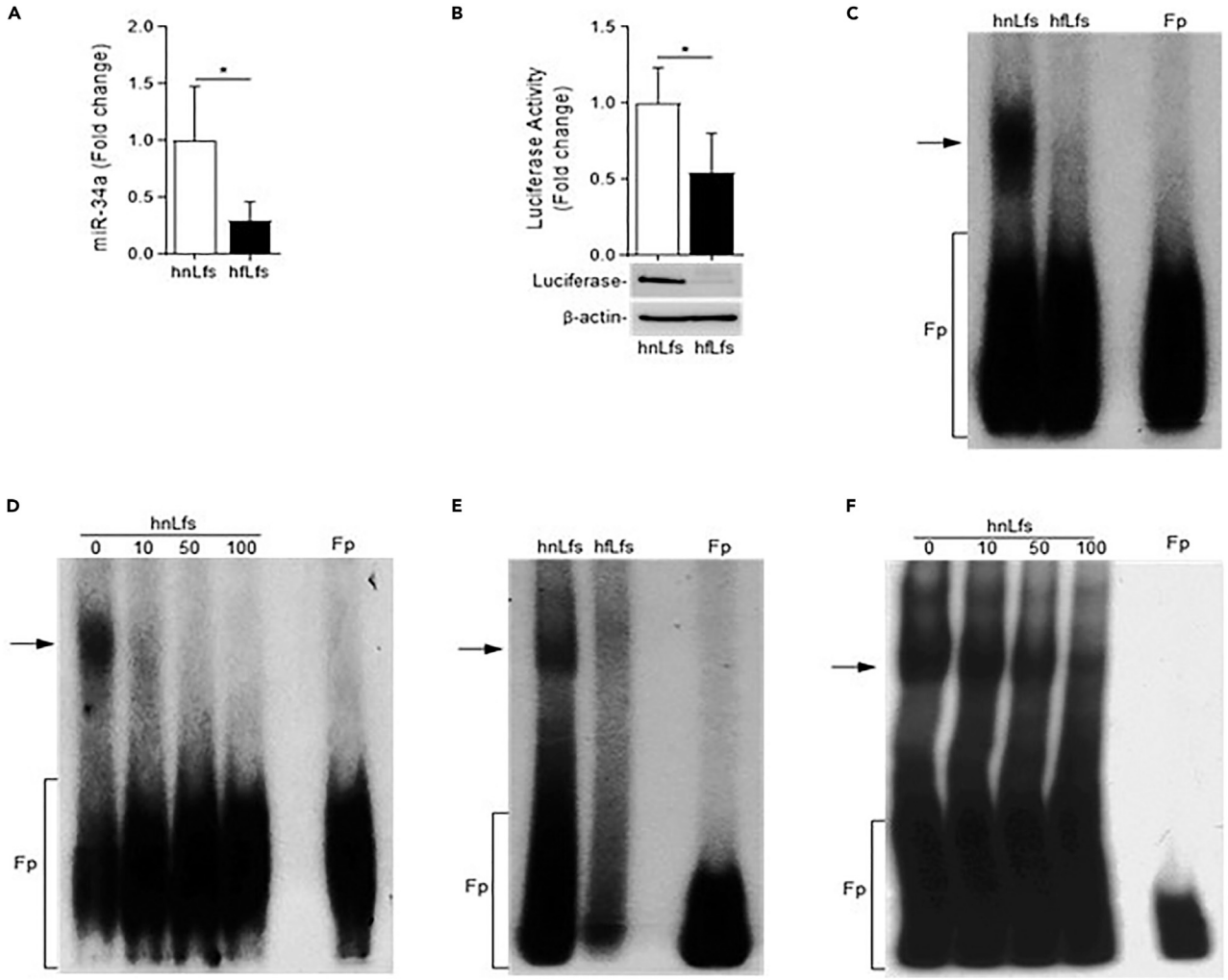

Figure 1. Disparate expression of miR-34a by nLfs and fLfs

(A) miR-34a expression normalized to U6 snRNA in hnLfs (n = 5) and hfLfs (n = 5) by qRT-PCR. Data are mean ± SD *p < 0.05 by Student's t test.

(B) hnLfs and hfLfs were transfected with miR-34a promoter binding sequence construct, harboring a luciferase reporter gene. Cell lysates were tested for luciferase activity using a chemiluminescence assay and immunoblotted for luciferase and β-actin protein (bottom of the bar graph). Data are mean ± SD (n = 4). *p < 0.05 by Student's t test.

(C and D) Gel mobility shift assay of hnLfs or hfLfs lysates using ^{32}P-labeled p53-binding promoter DNA consensus sequences in the absence and presence of 10, 50, and 100-fold molar excess of unlabeled promoter DNA consensus sequences. Fp = Free probe.

(E and F) Gel mobility shift assay of the hnLfs and hfLfs lysates using ^{32}P-labeled p53-binding chimeric uPA-uPAR-PAI-1 3′UTR mRNA sequences in the absence and presence of 10, 50, and 100-fold molar excess of unlabeled 3′UTR sequence. Fp = Free probe.

with the uPA-uPAR-PAI-1 3′UTR sequence was further confirmed by self-competition with a molar excess of unlabeled 3′UTR sequences (Figure 1F).

Because baseline miR-34a expression is lost in fLfs (Figure 1A), we treated nLfs with lentivirus expressing miR-34a antisense (Lv-miR-34a-AS) to test whether inhibition of miR-34a activates nLfs. Naive nLfs or nLfs transduced with lentivirus expressing empty vector (Lv-Ev) were used as controls. As shown in Figure 2A, inhibition of miR-34a reduced acetylated p53 (^{Ac}p53), total p53, and p53 downstream transcriptional and post-transcriptional target, PAI-1 while increasing Col1, FN, TN-C, and α-SMA protein, suggesting activation of nLfs. This was independently confirmed by increased basal expression of their mRNA, while decreasing the baseline PAI-1 mRNA in nLfs (Figure 2B). Because miR-34a controls cellular viability by causing growth arrest and senescence (Tazawa et al., 2007), we tested proliferation of Lv-miR-34a-AS transduced nLfs and compared the responses with naive nLfs and nLfs exposed to Lv-Ev. Consistent with loss of p53, because of suppression of miR-34a expression, we found that nLfs exposed to Lv-miR-34a-AS showed a significant

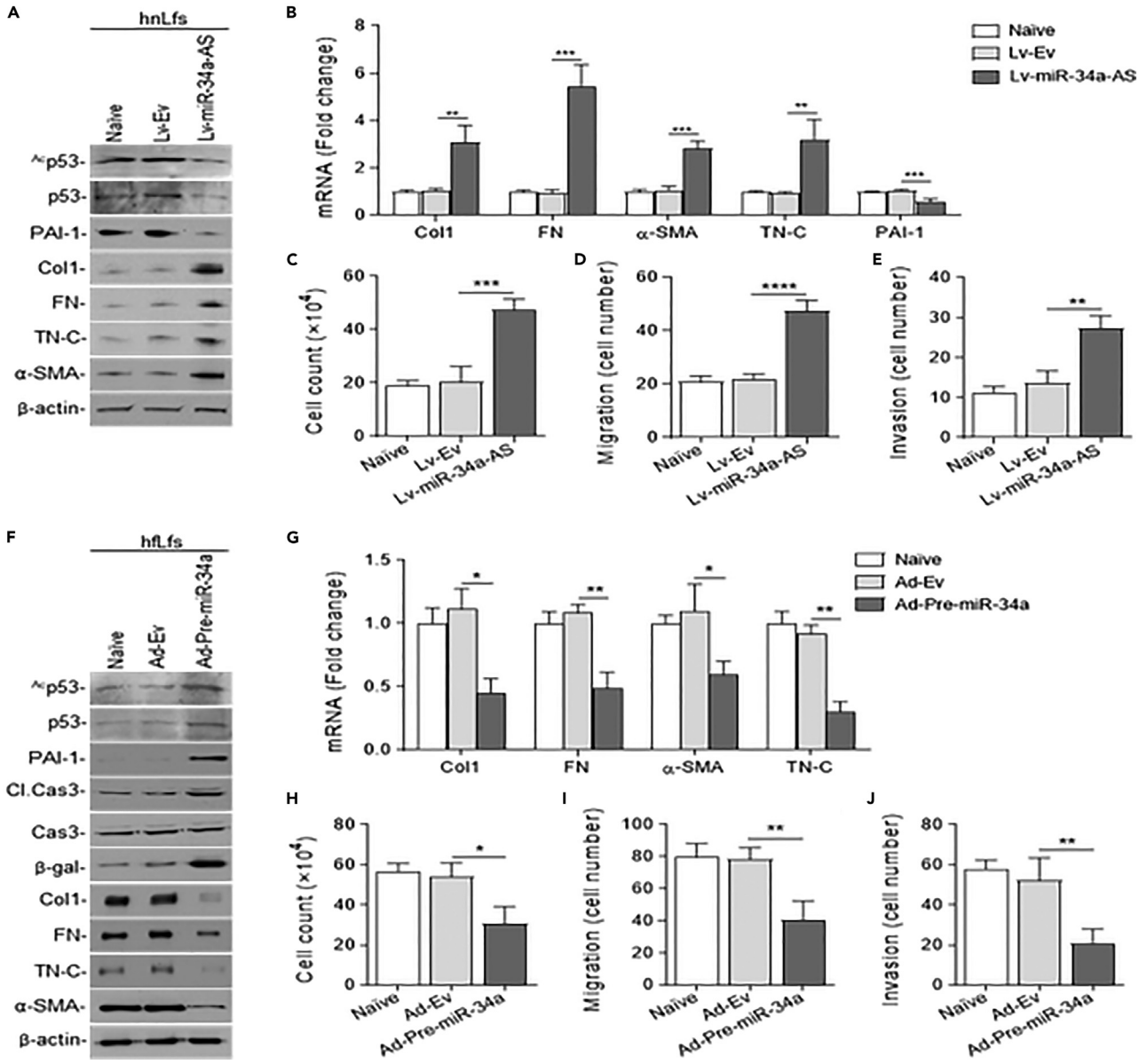

Figure 2. miR-34a regulates pro-fibrogenic phenotypes of Lfs

(A) Immunoblotting for p53, acetylated p53 (^{Ac}p53), PAI-1, and pro-fibrogenic marker proteins in naive human nLfs (hnLfs) or hnLfs transduced with Lv-Ev or Lv-miR-34a-AS.

(B) qRT-PCR for PAI-1 and pro-fibrogenic marker mRNAs in naive and transduced hnLfs as in (A).

(C–E) Proliferation (C), migration (D), and invasion (E) of naive and transduced hnLfs as in (A).

(F) Western blotting for ^{Ac}p53, p53, PAI-1, Cleaved/total caspase-3 (Cl. Cas3/Cas3), and pro-fibrogenic marker proteins in naive hfLfs and hfLfs transduced with Ad-Ev or Ad-Pre-miR-34a.

(G) qRT-PCR for pro-fibrogenic marker mRNAs in naive and transduced hfLfs as in (F).

(H–J) Proliferation (H), migration (I), and invasion (J) of naive and transduced hfLfs as in (F). Data are represented as mean ± SD from n = 3 experiments. *p < 0.05, **p < 0.01, and ***p < 0.001 (one-way ANOVA with Tukey's multiple-comparison test).

increase in the basal proliferation (Figure 2C). Similarly, inhibition of miR-34a in nLfs also caused an increase in migration (Figure 2D and Figure S1A) and invasion (Figure 2E) compared to naive or Lv-Ev treated nLfs.

To further confirm the role of miR-34a in dedifferentiation of fLfs, we transduced fLfs with adenovirus expressing precursor miR-34a (Ad-Pre-miR-34a). This led to increase in ^{Ac}p53, p53, and PAI-1, as well as

activation of caspase-3 and β-galactosidase (β-gal) expression (Figure 2F). This indicates an increase in senescence and apoptosis because of miR-34a-mediated restoration of p53 and PAI-1 expression in fLfs. These changes were associated with suppression of Col1, FN, TN-C and α-SMA proteins, and their mRNA (Figure 2G). Analyses of fLfs exposed to Ad-Pre-miR-34a showed significant reductions in the basal rate of proliferation (Figure 2H), migration (Figure 2I and Figure S1B), and invasion (Figure 2J). Ad-Pre-miR-34a transduction upregulated miR-34a in fLfs (Figure S2), implying the dedifferentiation of fLfs through restoration of basal miR-34a expression.

p53 induces miR-34a transcription by direct binding to promoter sequences, whereas miR-34a promotes p53 stabilization through inhibiting Sirt1 mRNA translation and consequent Sirt1-mediated deacetylation of p53 (Yamakuchi and Lowenstein, 2009). p53 and miR-34a expression are lost in fLfs (Figure 1) and forced expression of miR-34a restores p53 (Figure 2F). Therefore, we transduced human fLfs (hfLfs) isolated from IPF lungs with Lv-miR-34a-AS in the presence of adenovirus expressing p53 (Ad-p53). As shown in Figure 3A, transduction of hfLfs with Lv-miR-34a-AS further reduced the already low baseline expression of p53 in these cells. Consistent with increasing Sirt1 expression in fLfs exposed to Lv-miR-34-AS, ^{Ac}p53 was further reduced below baseline levels, suggesting increased Sirt1-mediated deacetylation of p53. This was associated with a further decline in PAI-1, active caspase-3, and β-gal, indicating resistance to apoptosis and senescence. Interestingly, restoration of p53 through Ad-p53 in Lv-miR-34a-AS treated hfLfs did not increase ^{Ac}p53, apoptosis, or senescence. This suggests a dominant role of miR-34a-mediated acetylation and stabilization of p53 in regulating fLf viability. In addition, expression of p53 in Lv-miR-34a-AS treated hfLfs failed to inhibit pro-fibrogenic marker proteins (Figure 3B) and their mRNAs (Figure 3C). Consistent with the inability of Ad-p53 to completely block expression of pro-fibrogenic markers in Lv-miR-34a-AS exposed hfLfs, these cells also failed to significantly reduce baseline proliferation (Figure 3D), migration (Figure 3E), and invasion (Figure 3F).

We then transduced hfLfs with Ad-Pre-miR-34a in the presence of lentivirus expressing p53 shRNA (Lv-p53 shRNA) to block increased miR-34a-induced p53 expression. Naive hfLfs, hfLfs exposed to Ad-Pre-miR-34a alone or Ad-pre-miR-34a plus lentivirus expressing non-specific control shRNA (Lv-Ctrl shRNA) were used as controls. As shown in Figure 3G, transduction of fLfs with Ad-Pre-miR-34a increased ^{Ac}p53, p53, and PAI-1 and reduced Sirt1 expression in fLfs. These changes also increased baseline apoptosis and senescence in these cells. This was reversed, following inhibition of miR-34a-induced p53 expression, by treating Ad-Pre-miR-34a exposed fLfs with Lv-p53 shRNA. Further analysis of these cells revealed that restoration of miR-34a expression in fLfs reduced the expression of pro-fibrogenic marker proteins (Figure 3H) and their mRNAs (Figure 3I). These changes were associated with a significant decrease in the basal rate of proliferation (Figure 3J), migration (Figure 3K), and invasion (Figure 3L) in fLfs exposed to Ad-Pre-miR-34a. This was reversed after inhibition of p53 expression, using Lv-p53 shRNA in Ad-Pre-miR-34a treated fLfs.

Because miR-34a and p53 regulate PDGFR-β and Sirt1 expression, we analyzed their baseline levels in nLfs and fLfs. Consistent with the loss of both p53 and miR-34a, we found that basal expression of these proteins was remarkably increased in fLfs with concurrent induction of Sirt1-mediated deacetylation and degradation of p53 (Figure 4A). In addition, fLfs showed remarkable increase in phosphorylation of Stat3 (pStat3) and suppression of protein phosphatase 2A catalytic (PP2Ac) subunit expression, suggesting loss of PP2A activity in fLfs. To confirm that miR-34a regulates PDGFR-β expression through Sirt1-mediated deacetylation and degradation of p53, we transduced hnLfs with Lv-miR-34a-AS and found that inhibition of baseline miR-34a expression reduced both ^{Ac}p53 and total p53 (Figure 2A). This resulted in elevated Sirt1, PDGFR-β, and pStat3 with loss of PP2Ac expression in nLfs. On the contrary, forced expression of miR-34a reduced both Sirt1, PDGFR-β, and pStat3, which were otherwise markedly increased in fLfs, and also restored baseline PP2Ac expression (Figure 4B). We next subjected hnLfs and hfLfs to a miR-34a pull-down assay. hnLfs and hfLfs were transduced with biotin-labeled miR-34a. Later, RNA associated with biotin-labeled miR-34a from these cells were precipitated down using streptavidin-coated magnetic beads. As shown in Figure 4C, transduction of hnLfs and hfLfs with biotin-labeled miR-34a increased precipitation of miR-34a with streptavidin beads compared to the corresponding levels in naive hnLfs or hfLfs. We further found that both PDGFR-β and Sirt1 mRNA were co-purified with biotin-labeled miR-34a, indicating their direct interactions in nLfs and fLfs. Because expression of miR-34a in fLfs inhibits pro-fibrogenic phenotypes, PDGFR-β and Sirt1, through induction of baseline p53, we transduced WT mice with BLM-induced existing PF with Ad-vector harboring FST1 promoter upstream of Pre-miR-34a or p53 to express in Lfs as we described elsewhere (Nagaraja et al., 2018). Analysis of whole lung homogenates for total

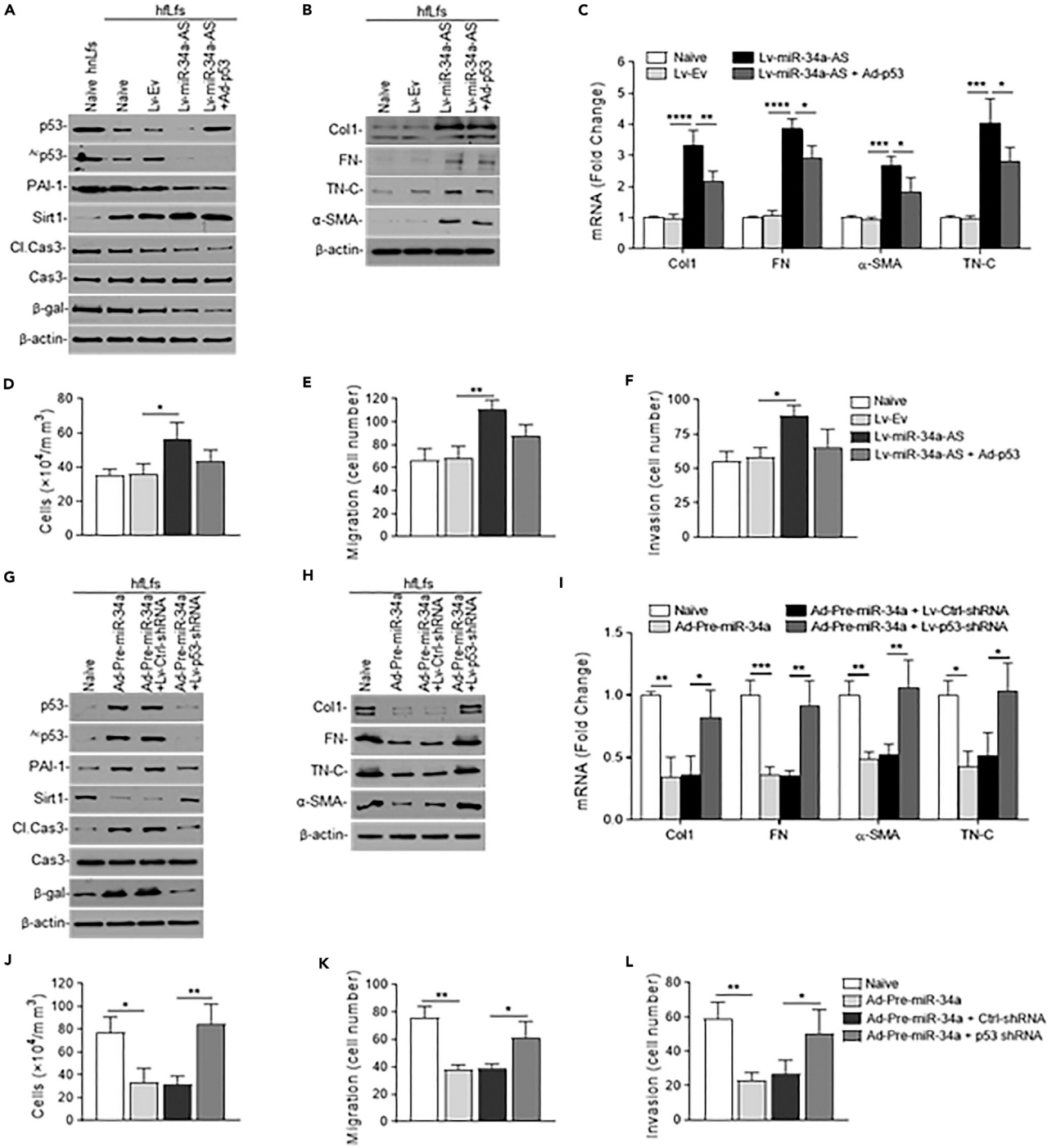

Figure 3. Role of p53 in miR-34a-mediated control of pro-fibrogenic phenotypes in lung fibroblasts

(A) Western blotting for p53, ^{Ac}p53, PAI-1, Sirt1, Cl. Cas3/Cas3 and β-gal protein in naive hnLfs, hfLfs, and hfLfs transduced with Lv-Ev, Lv-miR-34a-AS, or Lv-miR-34a-AS with Ad-p53.

(B and C) Naive hnLfs, or hfLfs transduced with Lv-Ev, Lv-miR-34a-AS, or Lv-miR-34a-AS with Ad-p53 as in (A) were analyzed for pro-fibrogenic marker protein (B) and mRNA (C).

(D–F) Proliferation (D), migration (E), and invasion (F) of naive hfLfs and hfLfs transduced as in (A).

(G) Western blotting for p53, ^{Ac}p53, PAI-1, Sirt1, Cl. Cas3/Cas3 and β-gal in naive hfLfs, and hfLfs transduced with Ad-Pre-miR-34a with or without Lv-control shRNA (Ctrl-shRNA) or Lv-p53-shRNA.

(H and I) Pro-fibrogenic marker protein (H) and mRNA (I) in naive and transfected hfLfs as in (G).

(J–L) Proliferation (J), migration (K), and invasion (L) of naive and transfected hfLfs as in (G). Data are mean ± SD from n = 3 experiments. *$p < 0.05$, **$p < 0.01$, ***$p < 0.001$, and ****$p < 0.0001$ (one-way ANOVA with Tukey's multiple-comparison test).

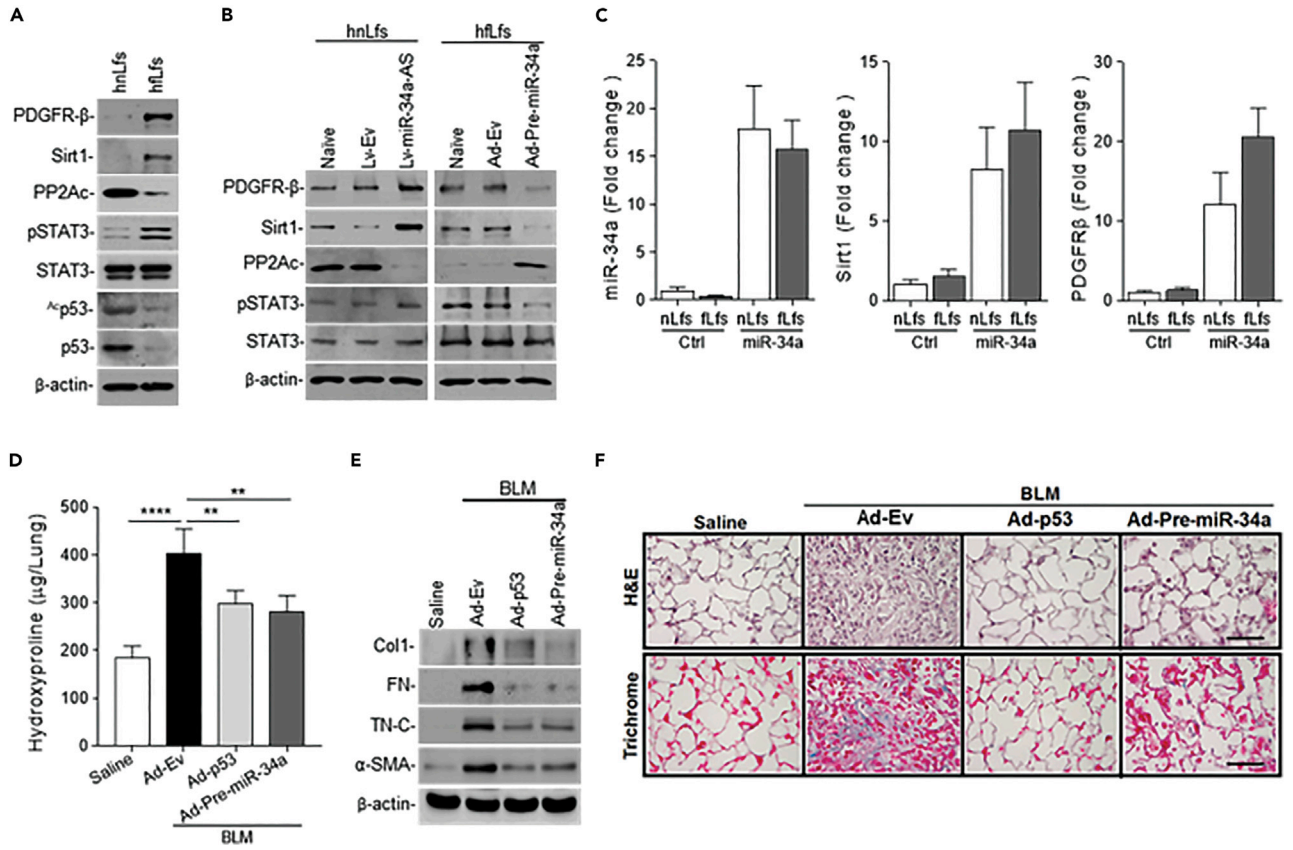

Figure 4. miR-34a mitigates PDGFR-β and Sirt1 in hfLfs, and in mice with BLM-induced PF

(A) Western blotting for PDGFR-β, Sirt1, PP2Ac, pStat3/Stat3, ^{Ac}p53, p53 in naive hnLfs and hfLfs.

(B) Western blotting of lysates from naive hnLfs and hnLfs transduced with Lv-Ev or miR-34a-AS as in (2A), naive hfLfs and hfLfs transduced with Ad-Ev or Pre-miR-34a as in (2F) for p53, ^{Ac}p53, PDGFR-β, PP2Ac, pStat3/Stat3, and Sirt1.

(C) The lysates of hnLfs and hfLfs transfected with or without biotin-labeled miR-34a were incubated with streptavidin-coated magnetic beads. The pulled down RNA was analyzed for miR-34a, PDGFR-β, and Sirt1 mRNA by qRT-PCR. mRNA level was normalized to the corresponding level in control cells. Data are mean ± SD from n = 3 experiments.

(D–F) WT mice were exposed to saline or BLM, 14 days later mice with BLM-PF were transduced with adenovirus vector harboring FTS1 promoter (Ad-Ev) or Ad-FTS1 vector expressing p53 (Ad-p53) or Pre-miR-34a via the airway. Mice were euthanized 21 days post-BLM exposure with whole lung homogenates analyzed. (D) Total hydroxyproline in lung homogenates (Data are mean ± SD n = 4 per group. **$p < 0.01$ and ****$p < 0.0001$ (one-way ANOVA with Tukey's multiple-comparison test). (E) Western blotting of pro-fibrogenic proteins in lung homogenates. (F) The inflated lung sections of mice treated as in (D) were subjected to H&E and trichrome staining to assess collagen and other ECM protein deposits. Scale bars, 100 μm.

hydroxyproline content (Figure 4D) or immunoblotting for pro-fibrogenic marker proteins (Figure 4E), demonstrated significant reduction in existing PF in WT mice exposed to either Ad-p53 or Ad-Pre-miR-34a. The results of H&E and trichrome staining of lung sections of WT mice further confirmed that forced expression of either p53 or miR-34a in Lfs markedly reduced BLM-induced PF (Figure 4F).

Anti-fibrogenic effects of CSP or CSP7 involves restoration of baseline expression of p53 in fLfs (Marudamuthu et al., 2019; Nagaraja et al., 2018). p53 is known to induce miR-34a transcription (Raver-Shapira et al., 2007). Therefore, we treated both hnLfs and hfLfs with either CSP or control peptide (CP) of scrambled sequence. As shown in Figure 5A, treatment of fLfs from IPF lungs with CSP increased miR-34a expression, whereas nLfs did not respond to CSP treatment. We further found that CSP7 caused a dose-dependent increase in miR-34a, while suppressing Col1 expression in hfLfs (Figure S3). To further confirm CSP7 increases miR-34a promoter activation in fLfs, we transduced nLfs and fLfs with miR-34a-luciferase promoter reporter constructs. The lysates were immunoblotted for luciferase antigen expression. Consistent with low miR-34a expression, we found a marked reduction in luciferase antigen expression in fLfs compared to baseline promoter activity in nLfs. This was increased in fLfs treated with CSP7, whereas those exposed to CP showed low level of luciferase protein (Figure 5B). Because p53 binds to miR-34a

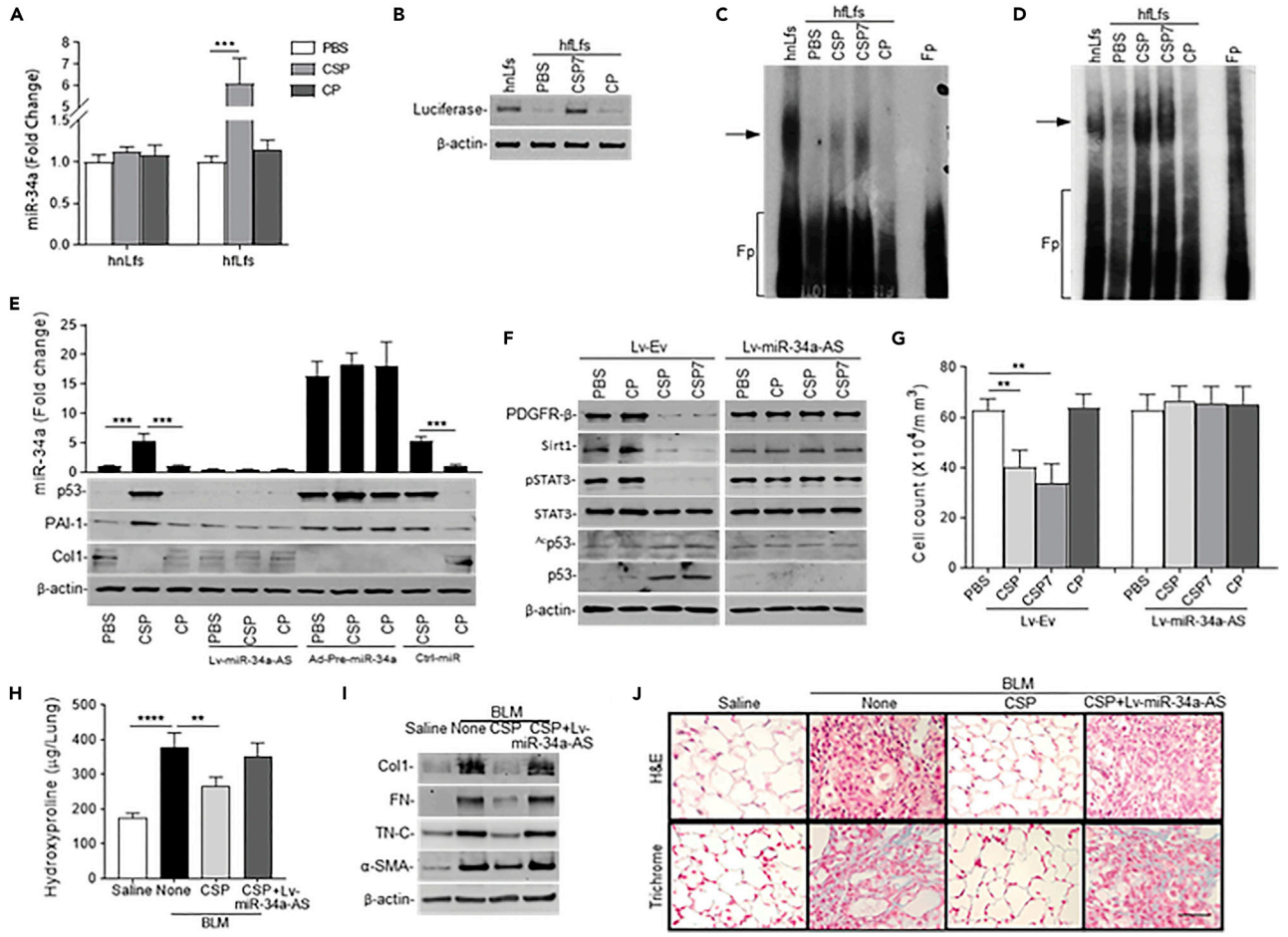

Figure 5. miR-34a-p53-feedback induction controls anti-fibrogenic effects of CSP or CSP7

(A) miR-34a expression in hnLfs and hfLfs treated with PBS, CSP, or CP. Data are mean ± SD from n = 3 experiments. ***p < 0.001 by one-way ANOVA with Tukey's multiple-comparison test.

(B) hnLfs and hfLfs were transduced with miR-34a promoter and luciferase reporter construct as in (1B). Luciferase protein expression in hnLfs, hfLfs, and hfLfs treated with CSP7 or CP.

(C) The lysates of hnLfs, and hfLfs treated with PBS, CSP, CSP7, or CP were subjected to gel mobility shift assay using ^{32}P-labeled p53-binding promoter DNA consensus sequences as in (1C).

(D) Lysates of hnLfs and hfLfs treated as in (C) were subjected to gel mobility shift assay using ^{32}P-labeled chimeric uPA-uPAR-PAI-1 3′UTR mRNA sequences as in (1E).

(E) hfLfs transduced with or without Lv-miR-34a-AS, Ad-Pre-miR-34a, or nonspecific control miRNAs (Ctrl-miR) were treated with PBS or CSP or CP. The lysates were tested for miR-34a by qRT-PCR and immunoblotted for Col1, PAI-1, p53, and β-actin (bottom of the bar graph). Data are mean ± SD from n = 3 experiments. ***p < 0.001 by one-way ANOVA with Tukey's multiple-comparison test.

(F) The lysates from hfLfs treated with PBS, CSP, CSP7, or CP in the presence of Lv-Ev or Lv-miR-34a-AS were immunoblotted for PDGFR-β, Sirt1, pStat3/Stat3, ^{Ac}p53, p53, and β-actin.

(G) hfLfs treated as in (F) were tested for total number of cells. Data are mean ± SD from n = 3 experiments. **p < 0.01 by one-way ANOVA with Tukey's multiple-comparison test.

(H–J) WT mice were exposed to saline or BLM. After 12 days, mice exposed to BLM were left untreated (None) or transduced with Lv expressing miR-34a-AS under the control of FTS1 promoter. Two days post-Lv-miR-34a-AS transduction, Lv-Ev and Lv-miR-34a-AS exposed mice were treated with CSP. (H) Hydroxyproline content in whole lung homogenates. Data are mean ± SD (n = 4 per group). **p < 0.01 and ****p < 0.0001 by one-way ANOVA with Tukey's multiple-comparison test. (I) Pro-fibrogenic marker proteins in lung homogenates by Western blotting. (J) Lung sections were subjected to H&E and trichrome staining. Scale bars, 100 μm.

promoter sequences and activates its expression, we subjected the lysates to a gel mobility shift assay using p53 promoter consensus sequences. Consistent with miR-34a promoter activation, we found nLf lysates showed robust baseline binding with p53 promoter consensus sequences. This was remarkably reduced in lysates from fLfs and improved in those treated with either CSP or CSP7 (Figure 5C), suggesting restoration

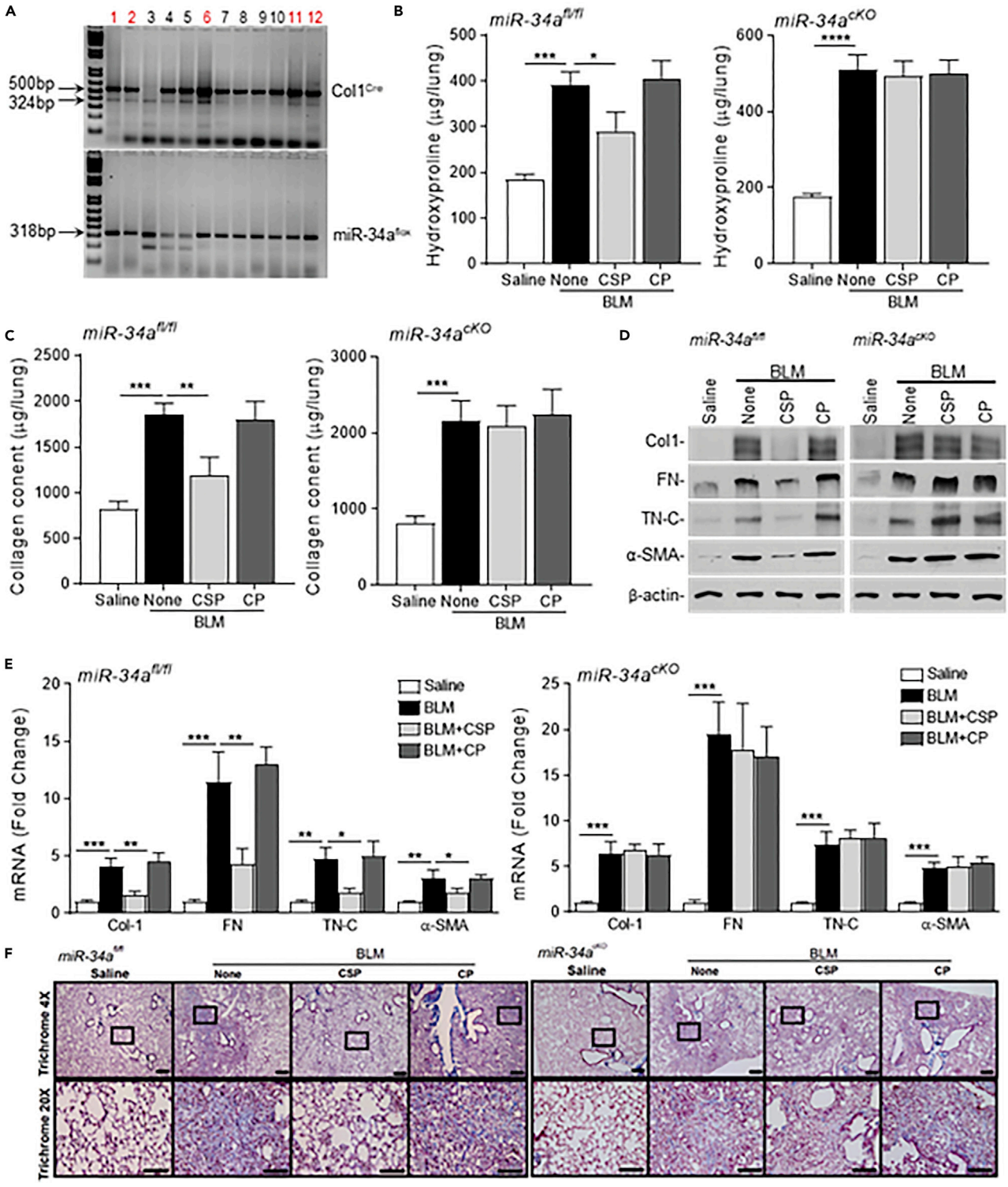

Figure 6. miR-34a^{cKO} mice lacking miR-34a expression in Lfs resist CSP treatment

(A) Crossbreeding of *miR-34a*$^{fl/fl}$ and *Col1*^{Cre} mice.

(B–F) *miR-34a*$^{fl/fl}$ and *miR-34a*^{cKO} (lane 1, 2, 6, 11, and 12) mice were treated with tamoxifen to induce cre recombinase. These mice were later exposed to saline or BLM. After 14 days miR-34a$^{fl/fl}$ and miR-34a^{cKO} mice exposed to BLM were IP injected with or without CSP or CP daily for 7 days. Twenty-one days after BLM, mice were euthanized. Whole lung homogenates were analyzed for (B) total hydroxyproline, (C) soluble collagen contents, (D) pro-fibrogenic

Figure 6. *Continued*
marker protein by Western blotting, and (E) pro-fibrogenic marker mRNA by qRT-PCR. (F) Sections of inflated lungs were subjected to Trichrome staining for collagen and related ECM protein. Scale bars, 50 μm, ×4 and 100 μm, ×20. Data are represented as mean ± SD (n = 3 per group). *p < 0.05, **p < 0.01, ***p < 0.001, and ****p < 0.0001 (one-way ANOVA with Tukey's multiple-comparison test).

of p53 expression following treatment with Cav1-derived peptides. We previously reported that p53 binds to uPA, uPAR, and PAI-1 mRNA 3′UTR determinants to regulate their expression. Therefore, we subjected lysates of hnLfs and hfLfs for 3′UTR mRNA binding. Consistent with the results shown in Figure 1E, lysates of hfLfs exhibited minimal binding with p53-binding chimeric uPA, uPAR, and PAI-1 mRNA 3′UTR sequences, compared to the baseline binding observed using nLf lysates. However, treatment of hfLfs with either CSP or CSP7 caused a robust increase in the mRNA binding activity (Figure 5D), suggesting increased p53 expression after treatment with CSP or CSP7.

hfLfs were treated with CSP in the presence of Lv-miR-34a-AS or Ad-Pre-miR-34a (Figure 5E). Treatment of hfLfs with CSP caused a significant increase in basal miR-34a expression. However, treatment of cells with CSP in the presence of Lv-miR-34a-AS blocked CSP-mediated induction of miR-34a expression in fLfs, whereas treatment of Ad-Pre-miR-34a transduced fLfs with CSP showed added effect. Western blotting of hfLf lysates for Col1 showed inhibition of Col1 expression consistent with induction of baseline miR-34a. These changes were associated with a parallel increase in p53 and its downstream target PAI-1 expression, suggesting the involvement of p53-miR-34a feedforward induction of PAI-1. Because both PDGFR-β and Sirt1 expression are increased in fLfs, and p53 and miR-34a regulate their expression, we analyzed the lysates of hfLfs treated with CSP or CSP7. All these induce p53 level by interfering mdm2 interaction with p53. As shown in Figure 5F, restoration of p53 expression by treatment with CSP or CSP7, inhibited PDGFR-β and Sirt1 expression. This was abolished following suppression of baseline p53 in fLfs through blockade of miR-34a expression using miR-34a-AS. Further, blockade of miR-34a expression also neutralized the abilities of CSP or CSP7 to mitigate fLf proliferation (Figure 5G). To further confirm the role of miR-34a in the anti-fibrogenic responses of CSP *in vivo*, we transduced WT mice with lentivirus harboring the FTS1 promoter upstream of miR-34a-AS 12 days post-BLM exposure. Mice exposed to BLM alone or BLM with miR-34a-AS were treated with CSP by intraperitoneal (IP) injection daily for 7 days starting day 14 post-BLM injury. All mice were euthanized 21 days after BLM exposure. Whole lung homogenates were analyzed for total hydroxyproline content, which showed that treatment with CSP reduced PF, and this was abrogated following blocked of miR-34a in lung fibroblasts by transduction of these mice with miR-34a-AS (Figure 5H). This was independently confirmed by further analysis of lung homogenates for pro-fibrogenic markers by Western blotting (Figure 5I). H&E and Trichrome staining of lung sections proved that WT mice treated with CSP limits PF, and this was abolished following inhibition of miR-34a in lung fibroblasts of these mice using miR-34-AS (Figure 5J).

Conditional knockout mice lacking miR-34a (miR-34a^{cKO}) in fibroblasts were produced by cross-breeding miR-34a$^{fl/fl}$ mice with Col^{Cre} mice. miR-34a$^{fl/fl}$ and miR-34a^{cKO} mice (Figure 6A) were later IP injected with tamoxifen to suppress miR-34a expression in fibroblasts by causing induction of Cre-recombinase. These mice were later exposed to BLM to induce PF. miR-34a$^{fl/fl}$ and miR-34a^{cKO} mice with BLM-induced PF were consecutively treated with vehicle, CSP, or CP for 7 days by IP injection. Analysis of whole lung homogenates of miR-34a$^{fl/fl}$ and miR-34a^{cKO} mice revealed that BLM caused significant PF in both strains of mice. Interestingly, miR-34a$^{fl/fl}$ mice with existing PF responded to CSP treatment, whereas miR-34a^{cKO} mice resisted CSP treatment (Figure 6B). Further, analysis of these lung homogenates for soluble collagen also demonstrated a significant reduction in CSP treated miR-34a$^{fl/fl}$ and not miR-34a^{cKO} mice with existing PF (Figure 6C). This unequivocally suggests that CSP-mediated restoration of miR-34a expression in lung fibroblasts is required for resolution of existing PF. This conclusion was further supported by the findings from Western blot (Figure 6D) and qRT-PCR (Figure 6E) analysis of lung homogenates for pro-fibrogenic markers. Histological examination of both H&E and Trichrome stained lung sections further demonstrated increased collagen and other ECM deposits in miR-34a$^{fl/fl}$ mice because of BLM-induced PF, which was remarkably absent following treatment of miR-34a$^{fl/fl}$ mice with CSP for 7 days (Figure 6F). These changes were resisted in miR-34a^{cKO} mice with BLM-induced PF.

DISCUSSION

IPF is the most common chronic ILD, which is progressive and fatal with an estimated incidence of 40-50 cases for 100,000 individuals in the United States (Esposito et al., 2015). The prognosis of patients with IPF is bleak with a median five-year survival of only 20% (Olson et al., 2007). Majority of patients present with advanced stage disease, well after respiratory symptoms are developed attributing at least in part to the poor survival. Aging, familial or genetic, male gender, environmental, occupational, and lifestyle

factors (particularly cigarette smoking) are known risk factors for IPF pathogenesis (King et al., 2011). Reduced AEC viability because of increased senescence and apoptosis is often associated with aging and increases susceptibility to develop PF. Mutations in surfactant proteins C and A, and telomerase are also known genetic causes for the development of PF. The morphometric studies have clearly established that sub-epithelial accumulation of fLfs, Col, and other ECM proteins forms a fibrotic focus of IPF lungs. Further, progressive expansion of the fibrotic foci into adjacent normal alveolar units by proliferation, migration, and invasion of fLfs results in irreversible scarring and obliteration of the lung parenchyma and alveolar space of the lungs required for gas exchange (Todd et al., 2012). Recent studies further link hyperplastic proliferation and release an array of growth factors, cytokines, and proteases by AECs because of repetitive alveolar epithelial injury to the activation of fLfs and progressive development of PF. Nevertheless, treatment with anti-inflammatory drugs has proven ineffective in mitigating established PF (Ahluwalia et al., 2014), suggesting fLfs are prime effectors of disordered repair. Although, multiple studies from our laboratory (Nagaraja et al., 2018) and others (Xia et al., 2008) using different mouse lung injury models and human IPF tissues demonstrated that resistance of fLfs to undergo apoptosis, and increased proliferation, migration, and invasion of fLfs contributes to their progressive and irreversible expansion. However, the mechanism contributing to the activation of fLfs is still unclear.

In a related vein, our recent studies suggest that the pro-fibrogenic phenotypic changes displayed by fLfs have at least in part been attributed to the loss of basal expression of tumor suppressor protein, p53 (Nagaraja et al., 2018). Using fLfs from patients with IPF and mice with BLM-induced PF, we now show that basal expression of miR-34a, a downstream transcriptional target of p53, is significantly reduced in fLfs, whereas HDAC, Sirt1, PDGFR-β, and pro-fibrogenic marker proteins such as Col1, α-SMA, FN and TN-C, and their mRNAs are markedly increased in fLfs. Restoration of miR-34a, which is lost because of low baseline expression of p53 in fLfs, inhibits Sirt1 and PDGFR-β, and reduces proliferation, migration, and pro-fibrogenic markers, indicating dedifferentiation of fLfs. Our data also show that low levels of p53 in fLfs is associated with low promoter DNA consensus sequences as well as uPA, uPAR, and PAI-1 mRNA 3′UTR sequences binding activities of p53. Inhibition of miR-34a in nLfs augments expression of Sirt1, PDGFR-β, and pro-fibrogenic marker proteins as well as rate of proliferation, migration, and invasion. The process was associated with concurrent Sirt1-mediated suppression of acetylation and total p53, and inhibition of p53-induced downstream PAI-1 expression. Forced expression of miR-34a in fLfs increased the accumulation of total p53, acetylated p53, and PAI-1 and inhibited Col1, α-SMA, FN, and TN-C, thereby suggesting an intricate link between baseline miR-34a level and pro-fibrogenic activity. Inhibition of miR-34a attenuated anti-fibrotic effects of forced expression of p53 in fLfs. Similarly, miR-34a failed to suppress pro-survival signals that promote proliferation, migration, and invasion in p53 shRNA treated fLfs. The data further reveals the interrelationship between p53 and miR-34a feedback induction in the control of lung fibroblast phenotypes.

We further found that treatment of fLfs with CSP or its deletion fragment, CSP7, augments miR-34a along with suppression of Sirt1 translation leading to increases in acetylated and total p53, and PAI-1. These changes were associated with concurrent increase in the p53 promoter binding and miR-34a promoter activation. In addition, miR-34a can inhibit PDGFR-β expression by directly binding to seed sequences in the 3′UTR of PDGFR-β mRNA (Garofalo et al., 2013). Further, Cav1 is known to induce p53 (Bartholomew et al., 2009; Galbiati et al., 2001), and both Cav1 and p53 block PDGFR-β signaling (Yamamoto et al., 1999; Yang et al., 2008), thereby inhibiting fLf proliferation and pro-fibrogenic responses. CSP and CSP7 also inhibit the production of Sirt1, PDGFR-β, Col1, and α-SMA as well as proliferation in fLfs, which were lost following miR-34a-AS-mediated suppression of miR-34a expression. These findings suggest that anti-fibrogenic effects of Cav1, CSP, or CSP7 are associated with restoration of basal expression of p53 and its transcriptional target miR-34a, which are otherwise lost in fLfs. These findings provide a proof-of-concept that suppression of fibrogenic properties of fLfs with CSP or CSP7 treatment or Cav1 expression possibly will occur through restoration of concurrent miR-34a-mediated induction of p53. The process involves increased acetylation of p53 and p53-mediated downstream induction of PAI-1 expression in fLfs. Interestingly, CSP or CSP7 protects AECs from stress-induced apoptosis and senescence in fibrotic lungs, and the process involves reduction in miR-34a and p53 expression which are otherwise augmented in injured AECs including IPF lungs (Shetty et al., 2017). This is further supported by the observation that miR-34a^{cKO} mice lacking its expression in AECs resist BLM-induced lung injury and development of PF (Cui et al., 2017b). Further, the inability of CSP to resolve BLM-induced existing PF in p53^{cKO} or miR-34a^{cKO} mice lacking p53 or miR-34a expression in fibroblasts further provide strong evidence that baseline miR-34a-p53 feedback induction controls fLf activation and PF. This involves miR-34a-mediated acetylation of p53 through inhibition of Sirt1 and PDGFR-β expression.

Further, our recent publications show Cav1 is increased in AECs harvested after BLM or cigarette smoke exposure-induced lung injury (Marudamuthu et al., 2015; Puthusseri et al., 2017). In the lung epithelium after BLM injury, the increment in Cav1 appears to regulate not only AEC apoptosis, but also growth arrest and senescence (Shivshankar et al., 2012). Cav1 expression also increases with aging and these effects potentiate epithelial injury, which prevents proper epithelial regeneration and stimulates fibrotic repair, especially in chronic, repetitive injury as occurs in IPF. Cav1 may exacerbate lung epithelial injuries, its loss of expression in the injured lung appears to protect against development of PF, where it exerts proapoptotic and antiproliferative effects on resident lung cells, including AECs and lung fibroblasts (Nagaraja et al., 2018; Shivshankar et al., 2012; Wang et al., 2006). We recently reported that CSP or CSP7 concurrently targets Cav1 in injured AECs because of its increased expression (Shetty et al., 2017), and mdm2 in fLfs for its relative overexpression and paucity of Cav1 in these cells (Nagaraja et al., 2018). Further, protection of AECs in injured fibrotic lungs by CSP or CSP7 (Bhandary et al., 2012, 2015; Marudamuthu et al., 2015, 2019; Shetty et al., 2012) underlie their ability to resolve existing PF with preservation of lung architecture and physiology. CSP7 resolves existing PF and improves lung function in WT mice when treated between day 14 through 21 after initiation of BLM-induced or Ad-TGF-β1-induced lung injury (Marudamuthu et al., 2019). This involves augmentation of Cav1 bioavailability including that attributable to CSP7 and inhibits pro-fibrogenic signaling. We and others have shown that CSP-based intervention can block lung inflammation and PF induced by BLM or TGF-β (Marudamuthu et al., 2019; Tourkina et al., 2008). Further, systemic delivery of CSP by IP injection or using osmotic pump as a pretreatment reduced pro-fibrogenic signaling including phospho (ph)-ERK, ph-Akt, ph-JNK near baseline control levels (Tourkina et al., 2008). This shows that a treatment designed to augment the bioavailability of Cav1 using CSP or CSP7 is salutary in these models, preserves AEC viability and restores normal lung architecture in this setting. Further, CSP or CSP7 neither suppress baseline Col1 and α-SMA nor induce p53 (Nagaraja et al., 2018) or miR-34a in hnLfs. Similarly, CSP7 does not induce p53 or apoptosis in uninjured AECs or normal lung tissues (Marudamuthu et al., 2019).

A recent study also suggests that the immune checkpoint protein PD-L1 is upregulated in invasive fLfs (Geng et al., 2019) and expression of PD-L1 is negatively regulated by p53 via elaboration of miR-34a (Cortez et al., 2016). Besides, suppression of either p53 or miR-34a augments expression of several proteins that are involved in proliferation, migration, and invasion in diverse cells. The activity and expression of protein tyrosine phosphatase 1B (PTP1B) can be suppressed by Sirt1. PTP1B regulates function of receptor tyrosine kinases such as EGFR and PDGFR-β, and intracellular Stat3 signaling pathways (Haj et al., 2002; Zabolotny et al., 2002). Consistent with these observations, we found an increased activation of Stat3 through tyrosine phosphorylation in fLfs. This was lost following treatment of fLfs with CSP or CSP7 further suggesting the involvement of increased acetylation of Stat3 because of inhibition of Sirt1-mediated deacetylation. Further, loss of PTP1B activity can contribute to inactivation of protein phosphatase 2A (PP2A) because of its increased phosphorylation by activated Src or other kinases, which is supported by the observation that PP2A activity is lost in fLfs (Bhandary et al., 2015). In addition, Stat3 acetylation can also induce its dephosphorylation via induction of Stat3 negative regulators such as SOCS1 and SOCS3 (Xiong et al., 2012), which in turn induces p53 and downstream augmentation of miR-34a and PAI-1 expression. Sirt1-mediated deacetylation can enhance binding of Akt and PDK1 to PIP3 and promote Akt signaling through increased phosphorylation in fLfs. It is well demonstrated that PI3K/Akt and FAK signaling are dysregulated because of loss of p53 provides survival and proliferative advantages to fLfs (Lim et al., 2008). Similarly, miR-34a-mediated inhibition of Sirt1 translation and consequent deacetylation of Akt by Sirt1 may result in increased acetylation of Akt and PDK1 leading to reduced binding of Akt to PIP3 and inhibition of Akt phosphorylation in CSP treated fLfs. Because ERK1/2 signaling occurs mostly downstream of EGFR and PDGFR-β signaling, it is possible that CSP or CSP7-mediated dephosphorylation of ERK1/2 (Tourkina et al., 2008) is secondary to inactivation of these growth factor receptors. This could affect CSP-mediated inhibition of fLf proliferation and survival by inactivation of ERK. This supports a causal link between baseline p53-miR-34a feedback and pro-fibrogenic phenotypes of fLfs. In addition, Cav1 inhibits Wnt signaling and β-catenin-mediated transcription, the activation of EGFR, MEK1, and ERK1/2 among other signaling intermediates (Galbiati et al., 2000).

miR-34a is not the only target of p53. miR-34a regulates cell viability and function independent of p53 by directly controlling the expression of proteins involved in cell cycle regulation. However, miR-34a–deficient mice develop more severe lung fibrosis than WT mice. Further, increased Sirt1 expression and Sirt1-mediated deacetylation because of loss of miR-34a-mediated suppression of Sirt1 translation contributes to mdm2-mediated degradation of p53 in fLfs, suggesting miR-34a could play a vital role fLf expansion. In addition, miR-34a is a direct transcriptional target of p53 and is markedly induced by

p53 (Raver-Shapira et al., 2007) and promotes p53-mediated cellular events (Fridman and Lowe, 2003). These observations prompted us to study the role of miR-34a in fibrotic diseases and anti-fibrotic responses of CSP7. In this study, we observed a significant reduction in the expression of miR-34a in fLfs isolated from IPF lungs. This is consistent with loss of baseline p53 and increased rates of proliferation, migration, and invasion often observed in expanding activated fLfs or myofibroblasts as reported in the literature. Although Cui and colleagues reported elevated miR-34a levels in primary Lfs from IPF lungs with higher senescence marker p21 (Cui et al., 2017a), cells undergoing senescence do not proliferate or actively expand. However, these cells resist apoptosis and acquire senescence associated secretory phenotype (SASP), which turns senescent cells into pro-inflammatory cells. Further, as reported in the literature PF, including IPF are highly diffused types of fibrotic disorders with morphologic changes include spatial and temporal heterogeneity incorporating areas of normal lung adjacent to diseased areas containing fLfs. Further, Lfs, including fLfs or myofibroblasts isolated from fibrotic lungs, including IPF lungs are highly heterogeneous because of various stages of differentiation, disease states, patient background and tissue microenvironment, and postharvest culture conditions (Thannickal et al., 2004). The fLfs we isolated from the patients with usual interstitial pneumonia (UIP) and exhibit elevated baseline rates of proliferation, migration, and invasion, which are often associated with loss of baseline p53 and its transcriptional target miR-34a. Based on these observations, we believe that Lfs with elevated miR-34a and senescence marker p21 reported by Cui et al. and ours are likely different with distinct function.

In summary, using primary fLfs isolated from fibrotic lungs of patients with IPF or mice with BLM-induced established PF, we demonstrate for the first time that restoring miR-34a and p53 feedback in fLfs by CSP or CSP7 intervention can inhibit aggressive fLf phenotypes *in vitro* and *in vivo*. The anti-fibrogenic activity of CSP or CSP7 is associated with inhibition of Sirt1 and PDGFR-β pathways and metabolic reprogramming through restoration of p53-miR-34a feedback induction in fLfs. Thus, activating Sirt1 signaling in injured AECs and its inhibition in fLfs through regulation of p53-miR-34a-feedback mechanism would promote alveolar epithelial regeneration and restraining of fLfs amplification required for resolution of PF. Ames testing for mutagenicity, *in vitro* and *in vivo* transformation assays and toxicity studies in multiple animal models indicated that CSP7 is safe. CSP7 is currently undergoing human phase 1 safety, tolerability, and pharmacokinetic trials in healthy volunteers (NCT04233814). We are hopeful that eventual testing in patients will determine the ultimate therapeutic potential implied here is translatable to patients with IPF or other PF.

Limitations of the study

FTS1 promoter can induce gene expression in alveolar macrophages and other lung resident cells besides lung fibroblasts. Similarly, tamoxifen treatment of *miR-34a*$^{fl/fl}$*Col*^{Cre} mice may inhibit miR-34a expression in macrophages and other cells besides fibroblasts. It is unclear whether CSP/CSP7 treatment resolves BLM-induced existing PF in aged mice and needs to be tested. Efficacy of CSP/CSP7 treatment and miR-34a overexpression in fLfs harboring p53 mutation can be taken up for further studies.

STAR★METHODS

Detailed methods are provided in the online version of this paper and include the following:

- KEY RESOURCES TABLE
- RESOURCE AVAILABILITY
  - Lead contact
  - Materials availability
  - Data and code availability
- EXPERIMENTAL MODEL AND SUBJECT DETAILS
  - Human lung fibroblasts
  - Lung fibroblast treatments
  - Animals
  - Mice treatments
- METHOD DETAILS
  - Western blotting and quantitative real time PCR
  - Gel mobility shift assays
  - Transduction
  - Biotinylated-miRNA-34a pulldown assay
  - Cell proliferation, migration, and invasion assays

- Hydroxyproline assay
- QUANTIFICATION AND STATISTICAL ANALYSIS

SUPPLEMENTAL INFORMATION

Supplemental information can be found online at https://doi.org/10.1016/j.isci.2022.104022.

ACKNOWLEDGMENTS

This work was supported in part by NIH grants R01HL133067 and HL151397, and FAMRI CIA Award 150063 to S.S.

AUTHOR CONTRIBUTIONS

Conceptualization, S.S.; Investigation, T.B.H, N.T., M.R.N., S.K.S., L.F., R.S., and Y.P.B; Writing – Original Draft, S.S.; Writing – Review & Editing, M.R.N., T.B.H., L.F., and S.S.; Visualization M.R.N. and L.F.; Supervisiion and Project Administration, S.S.; Funding Acquisition, S.S.

DECLARATION OF INTERESTS

S.S. has patents issued for the use of the caveolin-1 spanning domain and its fragments for the treatment of pulmonary fibrosis. S.S. is a consultant and investor of Lung Therapeutics, Inc., a University of Texas start-up biotechnology firm that is commercializing CSP7 for the treatment of IPF. All other authors declare no competing interests.

Received: June 30, 2021
Revised: December 2, 2021
Accepted: March 1, 2022
Published: April 15, 2022

REFERENCES

Ahluwalia, N., Shea, B.S., and Tager, A.M. (2014). New therapeutic targets in idiopathic pulmonary fibrosis. Aiming to rein in runaway wound-healing responses. Am. J. Respir. Crit. Care Med. *190*, 867–878. https://doi.org/10.1164/rccm.201403-0509PP.

Bartholomew, J.N., Volonte, D., and Galbiati, F. (2009). Caveolin-1 regulates the antagonistic pleiotropic properties of cellular senescence through a novel Mdm2/p53-mediated pathway. Cancer Res. *69*, 2878–2886. https://doi.org/10.1158/0008-5472.CAN-08-2857.

Bhandary, Y.P., Shetty, S.K., Marudamuthu, A.S., Fu, J., Pinson, B.M., Levin, J., and Shetty, S. (2015). Role of p53-fibrinolytic system cross-talk in the regulation of quartz-induced lung injury. Toxicol. Appl. Pharmacol. *283*, 92–98. https://doi.org/10.1016/j.taap.2015.01.007.

Bhandary, Y.P., Shetty, S.K., Marudamuthu, A.S., Gyetko, M.R., Idell, S., Gharaee-Kermani, M., Shetty, R.S., Starcher, B.C., and Shetty, S. (2012). Regulation of alveolar epithelial cell apoptosis and pulmonary fibrosis by coordinate expression of components of the fibrinolytic system. Am. J. Physiol. Lung Cell Mol. Physiol. *302*, L463–L473. https://doi.org/10.1152/ajplung.00099.2011.

Bhandary, Y.P., Shetty, S.K., Marudamuthu, A.S., Ji, H.-L., Neuenschwander, P.F., Boggaram, V., Morris, G.F., Fu, J., Idell, S., and Shetty, S. (2013). Regulation of lung injury and fibrosis by p53-mediated changes in urokinase and plasminogen activator inhibitor-1. Am. J. Pathol. *183*, 131–143. https://doi.org/10.1016/j.ajpath.2013.03.022.

Cortez, M.A., Ivan, C., Valdecanas, D., Wang, X., Peltier, H.J., Ye, Y., Araujo, L., Carbone, D.P., Shilo, K., Giri, D.K., et al. (2016). PDL1 Regulation by p53 via miR-34. J. Natl. Cancer Inst. *108*, djv303. https://doi.org/10.1093/jnci/djv303.

Cui, H., Ge, J., Xie, N., Banerjee, S., Zhou, Y., Antony, V.B., Thannickal, V.J., and Liu, G. (2017a). miR-34a inhibits lung fibrosis by inducing lung fibroblast senescence. Am. J. Respir. Cell Mol. Biol. *56*, 168–178. https://doi.org/10.1165/rcmb.2016-0163OC.

Cui, H., Ge, J., Xie, N., Banerjee, S., Zhou, Y., Liu, R.-M., Thannickal, V.J., and Liu, G. (2017b). miR-34a promotes fibrosis in aged lungs by inducing alveolarepithelial dysfunctions. Am. J. Physiol. Lung Cell Mol. Physiol. *312*, L415–L424. https://doi.org/10.1152/ajplung.00335.2016.

Esposito, D.B., Lanes, S., Donneyong, M., Holick, C.N., Lasky, J.A., Lederer, D., Nathan, S.D., O'Quinn, S., Parker, J., and Tran, T.N. (2015). Idiopathic pulmonary fibrosis in United States automated claims. Incidence, prevalence, and algorithm validation. Am. J. Respir. Crit. Care Med. *192*, 1200–1207. https://doi.org/10.1164/rccm.201504-0818OC.

Fridman, J.S., and Lowe, S.W. (2003). Control of apoptosis by p53. Oncogene *22*, 9030–9040. https://doi.org/10.1038/sj.onc.1207116.

Fridolfsson, H.N., Roth, D.M., Insel, P.A., and Patel, H.H. (2014). Regulation of intracellular signaling and function by caveolin. FASEB J. Off. Publ. Fed. Am. Soc. Exp. Biol. *28*, 3823–3831. https://doi.org/10.1096/fj.14-252320.

Galbiati, F., Volonte, D., Brown, A.M., Weinstein, D.E., Ben-Ze'ev, A., Pestell, R.G., and Lisanti, M.P. (2000). Caveolin-1 expression inhibits Wnt/beta-catenin/Lef-1 signaling by recruiting beta-catenin to caveolae membrane domains. J. Biol. Chem. *275*, 23368–23377. https://doi.org/10.1074/jbc.M002020200.

Galbiati, F., Volonte', D., Liu, J., Capozza, F., Frank, P.G., Zhu, L., Pestell, R.G., and Lisanti, M.P. (2001). Caveolin-1 expression negatively regulates cell cycle progression by inducing G0/G1 arrest via a p53/p21WAF1/Cip1-dependent mechanism. Mol. Biol. Cell *12*, 2229–2244.

Garofalo, M., Jeon, Y.-J., Nuovo, G.J., Middleton, J., Secchiero, P., Joshi, P., Alder, H., Nazaryan, N., Di Leva, G., Romano, G., et al. (2013). MiR-34a/c-Dependent PDGFR-α/β downregulation inhibits tumorigenesis and enhances TRAIL-induced apoptosis in lung cancer. PLoS ONE *8*, e67581. https://doi.org/10.1371/journal.pone.0067581.

Geng, Y., Liu, X., Liang, J., Habiel, D.M., Kulur, V., Coelho, A.L., Deng, N., Xie, T., Wang, Y., Liu, N., et al. (2019). PD-L1 on invasive fibroblasts drives fibrosis in a humanized model of idiopathic pulmonary fibrosis. JCI Insight *4*, e125326. https://doi.org/10.1172/jci.insight.125326.

Gomer, R.H., and Lupher, M.L. (2010). Investigational approaches to therapies for idiopathic pulmonary fibrosis. Expert Opin. Investig. Drugs *19*, 737–745. https://doi.org/10.1517/13543784.2010.484018.

Haj, F.G., Verveer, P.J., Squire, A., Neel, B.G., and Bastiaens, P.I.H. (2002). Imaging sites of receptor

dephosphorylation by PTP1B on the surface of the endoplasmic reticulum. Science *295*, 1708–1711. https://doi.org/10.1126/science.1067566.

King, T.E., Bradford, W.Z., Castro-Bernardini, S., Fagan, E.A., Glaspole, I., Glassberg, M.K., Gorina, E., Hopkins, P.M., Kardatzke, D., Lancaster, L., et al.; ASCEND Study Group (2014). A phase 3 trial of pirfenidone in patients with idiopathic pulmonary fibrosis. N. Engl. J. Med. *370*, 2083–2092. https://doi.org/10.1056/NEJMoa1402582.

King, T.E., Pardo, A., and Selman, M. (2011). Idiopathic pulmonary fibrosis. Lancet Lond. Engl. *378*, 1949–1961. https://doi.org/10.1016/S0140-6736(11)60052-4.

Liang, C.-C., Park, A.Y., and Guan, J.-L. (2007). In vitro scratch assay: a convenient and inexpensive method for analysis of cell migration in vitro. Nat. Protoc. *2*, 329–333. https://doi.org/10.1038/nprot.2007.30.

Lim, S.-T., Chen, X.L., Lim, Y., Hanson, D.A., Vo, T.-T., Howerton, K., Larocque, N., Fisher, S.J., Schlaepfer, D.D., and Ilic, D. (2008). Nuclear FAK promotes cell proliferation and survival through FERM-enhanced p53 degradation. Mol. Cell *29*, 9–22. https://doi.org/10.1016/j.molcel.2007.11.031.

Marudamuthu, A.S., Bhandary, Y.P., Fan, L., Radhakrishnan, V., MacKenzie, B., Maier, E., Shetty, S.K., Nagaraja, M.R., Gopu, V., Tiwari, N., et al. (2019). Caveolin-1-derived peptide limits development of pulmonary fibrosis. Sci. Transl. Med. *11*, eaat2848. https://doi.org/10.1126/scitranslmed.aat2848.

Marudamuthu, A.S., Bhandary, Y.P., Shetty, S.K., Fu, J., Sathish, V., Prakash, Y., and Shetty, S. (2015). Role of the urokinase-fibrinolytic system in epithelial-mesenchymal transition during lung injury. Am. J. Pathol. *185*, 55–68. https://doi.org/10.1016/j.ajpath.2014.08.027.

Nagaraja, M.R., Tiwari, N., Shetty, S.K., Marudamuthu, A.S., Fan, L., Ostrom, R.S., Fu, J., Gopu, V., Radhakrishnan, V., Idell, S., and Shetty, S. (2018). p53 expression in lung fibroblasts is linked to mitigation of fibrotic lung remodeling. Am. J. Pathol. *188*, 2207–2222. https://doi.org/10.1016/j.ajpath.2018.07.005.

Noble, P.W., and Homer, R.J. (2004). Idiopathic pulmonary fibrosis: new insights into pathogenesis. Clin. Chest Med. *25*, 749–758. https://doi.org/10.1016/j.ccm.2004.04.003.

Olson, A.L., Swigris, J.J., Lezotte, D.C., Norris, J.M., Wilson, C.G., and Brown, K.K. (2007). Mortality from pulmonary fibrosis increased in the United States from 1992 to 2003. Am. J. Respir. Crit. Care Med. *176*, 277–284. https://doi.org/10.1164/rccm.200701-044OC.

Phan, S.H. (2002). The myofibroblast in pulmonary fibrosis. Chest *122*, 286S–289S. https://doi.org/10.1378/chest.122.6_suppl.286s.

Puthusseri, B., Marudamuthu, A., Tiwari, N., Fu, J., Idell, S., and Shetty, S. (2017). Regulation of p53-mediated changes in the uPA-fibrinolytic system and in lung injury by loss of surfactant protein C expression in alveolar epithelial cells. Am. J. Physiol. Lung Cell Mol. Physiol. *312*, L783–L796. https://doi.org/10.1152/ajplung.00291.2016.

Raver-Shapira, N., Marciano, E., Meiri, E., Spector, Y., Rosenfeld, N., Moskovits, N., Bentwich, Z., and Oren, M. (2007). Transcriptional activation of miR-34a contributes to p53-mediated apoptosis. Mol. Cell *26*, 731–743. https://doi.org/10.1016/j.molcel.2007.05.017.

Richeldi, L., du Bois, R.M., Raghu, G., Azuma, A., Brown, K.K., Costabel, U., Cottin, V., Flaherty, K.R., Hansell, D.M., Inoue, Y., et al. (2014). Efficacy and safety of nintedanib in idiopathic pulmonary fibrosis. N. Engl. J. Med. *370*, 2071–2082. https://doi.org/10.1056/NEJMoa1402584.

Rothberg, K.G., Heuser, J.E., Donzell, W.C., Ying, Y.S., Glenney, J.R., and Anderson, R.G. (1992). Caveolin, a protein component of caveolae membrane coats. Cell *68*, 673–682. https://doi.org/10.1016/0092-8674(92)90143-z.

Shetty, S., Velusamy, T., Idell, S., Shetty, P., Mazar, A.P., Bhandary, Y.P., and Shetty, R.S. (2007). Regulation of urokinase receptor expression by p53: novel role in stabilization of uPAR mRNA. Mol. Cell Biol. *27*, 5607–5618. https://doi.org/10.1128/MCB.00080-07.

Shetty, S.K., Bhandary, Y.P., Marudamuthu, A.S., Abernathy, D., Velusamy, T., Starcher, B., and Shetty, S. (2012). Regulation of airway and alveolar epithelial cell apoptosis by p53-Induced plasminogen activator inhibitor-1 during cigarette smoke exposure injury. Am. J. Respir. Cell Mol. Biol. *47*, 474–483. https://doi.org/10.1165/rcmb.2011-0390OC.

Shetty, S.K., Tiwari, N., Marudamuthu, A.S., Puthusseri, B., Bhandary, Y.P., Fu, J., Levin, J., Idell, S., and Shetty, S. (2017). p53 and miR-34a feedback promotes lung epithelial injury and pulmonary fibrosis. Am. J. Pathol. *187*, 1016–1034. https://doi.org/10.1016/j.ajpath.2016.12.020.

Shivshankar, P., Brampton, C., Miyasato, S., Kasper, M., Thannickal, V.J., and Le Saux, C.J. (2012). Caveolin-1 deficiency protects from pulmonary fibrosis by modulating epithelial cell senescence in mice. Am. J. Respir. Cell Mol. Biol. *47*, 28–36. https://doi.org/10.1165/rcmb.2011-0349OC.

Suganuma, H., Sato, A., Tamura, R., and Chida, K. (1995). Enhanced migration of fibroblasts derived from lungs with fibrotic lesions. Thorax *50*, 984–989. https://doi.org/10.1136/thx.50.9.984.

Tazawa, H., Tsuchiya, N., Izumiya, M., and Nakagama, H. (2007). Tumor-suppressive miR-34a induces senescence-like growth arrest through modulation of the E2F pathway in human colon cancer cells. Proc. Natl. Acad. Sci. U S A *104*, 15472–15477. https://doi.org/10.1073/pnas.0707351104.

Thannickal, V.J., Toews, G.B., White, E.S., Lynch, J.P., and Martinez, F.J. (2004). Mechanisms of pulmonary fibrosis. Annu. Rev. Med. *55*, 395–417. https://doi.org/10.1146/annurev.med.55.091902.103810.

Todd, N.W., Luzina, I.G., and Atamas, S.P. (2012). Molecular and cellular mechanisms of pulmonary fibrosis. Fibrogenesis Tissue Repair *5*, 11. https://doi.org/10.1186/1755-1536-5-11.

Tourkina, E., Richard, M., Gööz, P., Bonner, M., Pannu, J., Harley, R., Bernatchez, P.N., Sessa, W.C., Silver, R.M., and Hoffman, S. (2008). Antifibrotic properties of caveolin-1 scaffolding domain *in vitro* and *in vivo*. Am. J. Physiol. Lung Cell Mol. Physiol. *294*, L843–L861. https://doi.org/10.1152/ajplung.00295.2007.

Wang, X.M., Zhang, Y., Kim, H.P., Zhou, Z., Feghali-Bostwick, C.A., Liu, F., Ifedigbo, E., Xu, X., Oury, T.D., Kaminski, N., and Choi, A.M.K. (2006). Caveolin-1: a critical regulator of lung fibrosis in idiopathic pulmonary fibrosis. J. Exp. Med. *203*, 2895–2906. https://doi.org/10.1084/jem.20061536.

Xia, H., Diebold, D., Nho, R., Perlman, D., Kleidon, J., Kahm, J., Avdulov, S., Peterson, M., Nerva, J., Bitterman, P., and Henke, C. (2008). Pathological integrin signaling enhances proliferation of primary lung fibroblasts from patients with idiopathic pulmonary fibrosis. J. Exp. Med. *205*, 1659–1672. https://doi.org/10.1084/jem.20080001.

Xiong, H., Du, W., Zhang, Y.-J., Hong, J., Su, W.-Y., Tang, J.-T., Wang, Y.-C., Lu, R., and Fang, J.-Y. (2012). Trichostatin A, a histone deacetylase inhibitor, suppresses JAK2/STAT3 signaling via inducing the promoter-associated histone acetylation of SOCS1 and SOCS3 in human colorectal cancer cells. Mol. Carcinog. *51*, 174–184. https://doi.org/10.1002/mc.20777.

Yamakuchi, M., and Lowenstein, C.J. (2009). MiR-34, SIRT1 and p53: the feedback loop. Cell Cycle *8*, 712–715. https://doi.org/10.4161/cc.8.5.7753.

Yamamoto, M., Toya, Y., Jensen, R.A., and Ishikawa, Y. (1999). Caveolin is an inhibitor of platelet-derived growth factor receptor signaling. Exp. Cell Res. *247*, 380–388. https://doi.org/10.1006/excr.1998.4379.

Yang, W., Wetterskog, D., Matsumoto, Y., and Funa, K. (2008). Kinetics of repression by modified p53 on the PDGF beta-receptor promoter. Int. J. Cancer *123*, 2020–2030. https://doi.org/10.1002/ijc.23735.

Zabolotny, J.M., Bence-Hanulec, K.K., Stricker-Krongrad, A., Haj, F., Wang, Y., Minokoshi, Y., Kim, Y.-B., Elmquist, J.K., Tartaglia, L.A., Kahn, B.B., and Neel, B.G. (2002). PTP1B regulates leptin signal transduction *in vivo*. Dev. Cell *2*, 489–495. https://doi.org/10.1016/s1534-5807(02)00148-x.

STAR★METHODS

KEY RESOURCES TABLE

REAGENT or RESOURCE	SOURCE	IDENTIFIER
Antibodies		
Mouse anti-Firefly luciferase	Thermo Fisher Scientific	Cat# MA1-12556; RRID: AB_1076533
Rabbit anti-PDGFRβ	Abcam	Cat# ab32570; RRID: AB_777165
Rabbit anti-Acetyl-p53 (Lys379)	Cell Signaling	Cat# 2570; RRID: AB_823591
Mouse anti-p53	Cell Signaling	Cat# 2524; RRID: AB_331743
Goat anti-PAI-1	Abcam	Cat# ab31280; RRID: AB_777019
Mouse anti-Stat3	Cell Signaling	Cat# 9139; RRID: AB_331757
Mouse anti-phospho-Stat3 (Tyr705)	Cell Signaling	Cat# 4113; RRID: AB_2198588
Rabbit anti-Cleaved Caspase-3	Cell Signaling	Cat# 9664; RRID: AB_2070042
Rabbit anti-Caspase-3	Cell Signaling	Cat# 9662; RRID: AB_331439
Goat anti-Type I Collagen	SouthernBiotech	Cat# 1310-01; RRID: AB_2753206
Mouse anti-Type I Collagen	Abcam	Cat# ab6308; RRID: AB_305411
Rabbit anti-Fibronectin	Abcam	Cat# ab2413; RRID: AB_2262874
Mouse anti-SirT1	Cell Signaling	Cat# 8469; RRID: AB_10999470
Rabbit Anti-PP2A C	Cell Signaling	Cat# 2259; RRID: AB_561239
Rabbit anti-Tenascin C	Cell Signaling	Cat# 12221; RRID: AB_2797849
Rabbit anti-α-SMA	Abcam	Cat# ab32575; RRID: AB_722538
Rabbit anti-β-Galactosidase	Cell Signaling	Cat# 27198; RRID: AB_2798940
Mouse anti-β-actin	Cell Signaling	Cat# 3700; RRID: AB_2242334
Peroxidase-AffiniPure Donkey Anti-Goat IgG	Jackson ImmunoResearch Labs	Cat# 705-035-147; RRID: AB_2313587
Peroxidase-AffiniPure Donkey Anti-Rabbit IgG	Jackson ImmunoResearch Labs	Cat# 711-035-152; RRID: AB_10015282
Peroxidase-AffiniPure Donkey Anti-Mouse IgG	Jackson ImmunoResearch Labs	Cat# 715-035-150; RRID: AB_2340770
Chemicals and Peptides		
Bleomycin sulfate	Biotang	RB003
Tamoxifen	Cayman chemical	13258
CSP, caveolin-1 scaffolding domain peptide	Genescript	Custom made
CSP7, 7-mer of CSP	Genescript	Custom made
CP, control peptide of scrambled sequence	Genescript	Custom made
tRNA from *E. coli*	Sigma	10109541001
T7 RNA Polymerase	Promega	P2075
Dynabeads Streptavidin	Thermo Fisher Scientific	11205D
Lipofectamine 2000	Thermo Fisher Scientific	11668019
RNase T1	Thermo Fisher Scientific	EN0452
Trypsin	Fisher Scientific	SH30236
Cell lines		
Human normal lung fibroblasts	This lab	
Human fibrotic lung fibroblasts (IPF)	Dr Cory Hogoboam, University of Michigan, Dr Ganesh Raghu, University of Washington	Gift
Critical commercial assays		
NCode™ EXPRESS SYBR® GreenER™ miRNA qRT-PCR Kit Universal	Invitrogen	A11193-051
Pierce™ Firefly Luciferase Glow assay kit	Thermo Fisher Scientific	16176

(*Continued on next page*)

Continued

REAGENT or RESOURCE	SOURCE	IDENTIFIER
24-well Transwell	Corning	3422
BD BioCoat™ BD Matrigel™ Invasion Chamber	BD Biosciences	354480
ImProm-II™ Reverse Transcription System	Promega	A3800
Power SYBR™ Green PCR Master Mix	Applied Biosystems	4367659
Trichrome Stain (Masson) Kit	Sigma	HT15-1KT
Experimental model: Organisms/strains		
Mouse: C57BL/6J	Mouse: C57BL/6J	Mouse: C57BL/6J
Mouse: *miR-34a*$^{fl/fl}$ (*Mir34a*$^{tm1.2Aven}$/J)	Mouse: *miR-34a*$^{fl/fl}$ (*Mir34a*$^{tm1.2Aven}$/J)	Mouse: *miR-34a*$^{fl/fl}$ (*Mir34a*$^{tm1.2Aven}$/J)
Mouse: B6.Cg-Tg(Col1a1-cre/ERT2)1Crm/J	Mouse: B6.Cg-Tg(Col1a1-cre/ERT2)1Crm/J	Mouse: B6.Cg-Tg(Col1a1-cre/ERT2)1Crm/J
Oligonucleotides		
miRNA inhibitor AAV particles	Genecopoeia	MmiR-AN0440-SN-10
uPA-uPAR-PAI-1 3'UTR chimera	Bhandary et al., 2013	
Vectors		
pGL3-PMT-miR-34a	Addgene	Plasmid #25799
miRNA scrambled control clone	Genecopoeia	CmiR0001-MR04
pSMPUW Lentiviral Expression Vector	Cell Biolabs	#VPK-211
RAPAd® Universal Adenoviral Expression System	Cell Biolabs	#VPK-250
Recombinant DNA		
Ad-p53	Nagaraja et al., 2018	
Ad-Pre-miR-34a	This paper	
Lv-miR-34a-AS	This paper	
p53 shRNA (h) Lentiviral Particles	Santa Cruz	sc-29435-V
Control shRNA Lentiviral Particles	Santa Cruz	sc-108080
Software and aligorithms		
Graphpad Prism 9.0.0	GraphPad Software	https://www.graphpad.com/

RESOURCE AVAILABILITY

Lead contact

Further information and requests for resources and reagents should be directed to and will be fulfilled by the lead contact, Sreerama Shetty (sreerama.shetty@uthct.edu).

Materials availability

In this study, two recombinant DNA viz., Ad-Pre-miR-34a and Lv-miR-34a-AS were generated

Data and code availability

- This paper does not report original code
- Any additional information required to reanalyze the data reported in this paper is available from the lead contact upon request

EXPERIMENTAL MODEL AND SUBJECT DETAILS

Human lung fibroblasts

Human nLfs and fLfs (IPF) were purchased from Cory Hogaboam (University of Michigan, Ann Arbor, Michigan, USA), provided by Ganesh Raghu (University of Washington, Seattle, Washington, USA), or isolated locally from control and IPF lung tissues as we described elsewhere (Marudamuthu et al., 2019). Patient demographics of all fibroblasts in this study are listed in Table S1. All hfLfs used in the study

were well characterized, derived from patients with usual interstitial pneumonia (UIP). To avoid heterogeneity associated with fLfs, we selected fLfs expressing elevated levels of profibrogenic marker proteins such as Col1, α-SMA, FN, and TN-C with minimal expression of Cav1, p53, and PAI-1. Human nLfs were derived from control donors without apparent interstitial or other lung diseases. Briefly, human lung tissues were minced and digested with 0.1% collagenase and 0.005% trypsin in Hanks' Balanced Salt Solution (HBSS) for 1 hour at 37 °C. Fibroblasts were selected by adherence of the suspension on cell culture dishes. The adherent lung fibroblasts were tested for profibrogenic phenotypes by analyzing Col1, α-SMA, FN, and TN-C, as well as Cav1 and p53 expression; cultured in DMEM containing 4.5 g/L D-Glucose, 10% FBS, and 1% penicillin and streptomycin at 37 °C; and used within 3–5 passages of initial isolation.

Lung fibroblast treatments

nLfs and fLfs cultured as above were treated with PBS, or 10 μM CSP or CSP7 or control peptide of scrambled sequence (CP) in the presence or absence of control (Ctrl)-miR or miR-34a-AS or Pre-miR-34a. The conditioned media were tested for Col1 and PAI-1 and the cell lysates were tested for ^{Ac}p53/p53, PDGFR-β, Sirt1 and β-actin. Total RNA was analyzed for miR-34a. The cell lysates were also subjected to gel mobility shift assay to assess p53 binding to promoter DNA and uPA-uPAR-PAI-1 3'UTR sequences. The lysates of nLfs and fLfs transduced with Ad-vector expressing miR-34a-luciferase reporter constructs and treated with PBS, CSP7 or CP were immunoblotted for luciferase antigen to assess miR-34a promoter activation.

Animals

Animal experiments described in the current study were approved by the Institutional Animal Care and Use Committee (IACUC). Six to eight weeks old wild-type (WT) C57BL/6 mice of both sexes weighing approximately 20-22g were purchased from The Jackson Laboratory (Bar Harbor, ME). Male and female miR-34a^{cKO} mice were generated by crossbreeding homozygous miR-34a floxed (*miR-34a*$^{fl/fl}$) mice with collagen Cre (*Col*^{Cre}) mice.

Mice treatments

Transduction of Ad-Pre-miR-34a and CSP treatment in BLM-induced PF mice

cDNA corresponding to miR-34a-AS or Ctrl-miR was cloned into a promoter-less Lv-pSMPUW Vector harboring fibroblast-specific protein promoter (FTS1) sequence as we described earlier (Nagaraja et al., 2018). Lv harboring promoter alone (Lv-Ev) was used as a vector control. For miR-34a overexpression, cDNA corresponding to Pre-miR-34a sequences was subcloned downstream of FST1 linked to the luciferase reporter gene into a pacAd5 K-N pA Ad vector (Ad) as we described earlier. WT mice were exposed to saline (50 μl) or BLM (8 U/kg) in saline via intranasal insufflation to induce PF. Twelve days after BLM exposure, some mice were exposed to Lv-Ev or Lv-miR-34a-AS and later treated with CSP (1.5 mg/kg) by intraperitoneal (IP) injection from day 14 through day 21 post-BLM as we described (Nagaraja et al., 2018). In a separate experiment, WT mice exposed to BLM were transduced with Ad-Ev or Ad-Pre-miR-34a 14 days after BLM exposure to target existing PF. All mice were euthanized 21 days post-BLM exposure and lung tissues were evaluated for changes in PF.

CSP7 treatment in miR-34a^{cKO} mice

Mice carrying mutant miR-34a and Col^{Cre} alleles were consecutively given IP injection of tamoxifen (75 mg/kg body weight) for 5 days to inhibit miR-34a expression in fibroblasts. miR-34$^{fl/fl}$ and miR-34a^{cKO} mice were exposed to either saline or BLM via nose as described above. Fourteen days later, BLM treated miR-34$^{fl/fl}$ and miR-34a^{cKO} mice were left untreated or treated with CSP7 or CP. All mice were euthanized 21 d after BLM lung injury and lungs were evaluated for changes in BLM-induced PF.

METHOD DETAILS

Western blotting and quantitative real time PCR

The cell lysates from nLfs and fLfs and mice lung homogenate were subjected to Western blotting as described elsewhere (Bhandary et al., 2012). RNA isolated from nLfs, fLfs and mice lung homogenate were also reverse transcribed and subjected to quantitative real-time PCR (qRT-PCR) for Col1, FN, α-SMA and TN-C transcripts as we described (Shetty et al., 2017). Mature miR-34a expression was quantified using NCode^{TM} EXPRESS SYBR GreenER^{TM} miRNA qRT-PCR Kit Universal (Invitrogen) according to the manufacturer's protocol. Briefly, RNA samples were polyadenylated and reverse transcribed, and then

cDNA was subjected to qRT-PCR using SYBR Green ER qRT-PCR Mix with miR-34a forward primer and Universal qRT-PCR Primer. Expression of miR-34a was normalized to U6 snRNA.

Gel mobility shift assays

To assess protein-promoter DNA binding

Total lysates (20 μg) from nLfs or fLfs, or fLfs treated with PBS, CSP, CSP7 or CP were subjected to DNA electrophoretic mobility shift assay (Bhandary et al., 2013). The specificity of p53-promoter DNA binding was confirmed by self-competition by incubation of nLf lysates with 0-100-fold molar excess of unlabeled promoter DNA before adding ^{32}P-labeled DNA probe into the reaction mixture.

For protein-3'UTR mRNA binding

RNA gel mobility shift was performed using p53-binding chimeric uPA-uPAR-PAI-1 3'UTR sequences as a probe as we described earlier (Bhandary et al., 2013; Shetty et al., 2007). Briefly, uniformly labeled chimeric uPA-uPAR-PAI-1 3'UTR transcripts were synthesized by *in vitro* transcription using linearized cDNA template containing uPA, uPAR and PAI-1 3'UTR sequences cloned in pcDNA3.1 vector, T7 RNA polymerase and ^{32}P-labeled UTP. The mRNA-protein binding reactions were performed at 30 °C by incubating ^{32}P-labeled chimeric mRNA transcripts (20,000 cpm) with cell extracts (20 μg) in 15 mM KCl, 5 mM $MgCl_2$, 0.25 mM EDTA, 0.25 mM Dithiothreitol, 12 mM HEPES pH 7.9, 10% Glycerol and *E. coli* tRNA (200 ng/μl) in a total volume of 20 μl at 30 °C for 30 min. The mRNA-protein reaction mixtures were treated with 50 units of RNase T1 and incubated for an additional 30 min at 37 °C. To avoid non-specific protein binding, 5 mg/ml Heparin was added, and the reaction mixture was incubated at room temperature for an additional 10 min. The ^{32}P-labeled mRNA-protein complexes were then separated on 5% native polyacrylamide gels, dried and auto-radiographed. The specificity of binding was confirmed by gel mobility shift assays with a ^{32}P-labeled chimeric mRNA transcript in the presence of a 0-100-fold molar excess of unlabeled 3'UTR mRNA transcripts of p53 binding sequence.

Transduction

nLfs and fLfs cultured as above, were treated with lentivirus (Lv) vector expressing miR-34a-AS (Lv-miR-34a-AS). Naïve nLfs and nLfs exposed to Lv expressing empty vector (Lv-Ev) were used as controls. fLfs were transduced with adenovirus (Ad) vector expressing precursor-miR-34a (Ad-Pre-miR-34a). Naïve fLfs and fLfs transduced with Ad-Ev were used as controls. The cell lysates were immunoblotted for p53, PAI-1 and fibrogenic markers. RNAs were tested for PAI-1 and pro-fibrogenic marker mRNAs. In separate experiments, equal numbers of naïve nLfs or nLfs exposed to Lv-Ev or Lv-miR-34a-AS, or naïve fLfs or fLfs transduced with Ad-Ev or Ad-Pre-miR-34a, were tested for proliferation, migration and invasion as we described the method earlier (Nagaraja et al., 2018).

To independently confirm the involvement of p53 and miR-34a feedforward induction in anti-fibrotic responses, fLfs were transduced with Lv-miR-34a-AS alone or Lv-miR-34a-AS was co-transduced with Ad vector expressing p53 (Ad-p53). Naïve nLfs and fLfs, or fLfs transduced with Ad-Ev were used as controls. fLfs were transduced with Ad-Pre-miR-34a alone or Ad-Pre-miR-34a co-transduced with Lv expressing p53 shRNA (Lv-p53 shRNA) to suppress miR-34a-induced p53. The control fLfs were exposed to Lv expressing non-specific control shRNA (Lv-Ctrl-shRNA). These cells were analyzed for p53, PAI-1 and fibrogenic marker proteins and their mRNAs as well as changes in the rate of proliferation, migration, and invasion.

Biotinylated-miRNA-34a pulldown assay

hnLfs and hfLfs were transfected with biotin-miR-34a. After 48h, cells were harvested and washed with ice-cold PBS, cell pellets were resuspended in 0.5 ml lysis buffer with protease inhibitor and RNase inhibitor, and incubated on ice for 5 min. The cytoplasmic lysate was isolated by centrifugation at 10,000×g for 10 min. Streptavidin-coated magnetic beads were blocked for 2h at 4°C in lysis buffer containing 1 mg/ml yeast tRNA and 1 mg/ml BSA and washed twice with 0.5 ml lysis buffer. Cytoplasmic lysate was added to the beads and incubated for 4h at 4°C before the beads were washed five times with 0.5 ml lysis buffer. RNA bound to the beads (pull-down RNA) was isolated using Trizol reagent. The level of mRNA in the biotin-miR-34a pull-down was quantified by qRT-PCR.

Cell proliferation, migration, and invasion assays

Cell proliferation, migration, and invasion assays were performed as we described earlier (Nagaraja et al., 2018). Equal numbers of hnLfs or hfLfs were seeded in 60-mm dishes and subjected to various treatments.

Five days later, cells were counted to assess the rate of proliferation. For fibroblast migration, transwell and scratch assays were performed. Transwell assays were performed in 6.5-mm–diameter Boyden chambers with a pore size of 8.0 mm. Lfs (1.0×10^5 cells per well) were resuspended in the DMEM without FBS and placed in the upper compartment of transwell chambers. The lower compartment was filled with DMEM containing 10% FBS as a chemoattractant. After incubation for 12h, Lfs on the lower surface of the filter were fixed in 4% formaldehyde and stained with 0.1% crystal violet. Five random fields were counted for each filter. Scratch assays were performed as described (Liang et al., 2007). Briefly, 48h after transfection, nLfs and fLfs at 90% confluence were scratched using a P200 pipette tip. Cells were washed, and then cultured with complete medium for an additional 18h with monitoring. Lf invasion was measured using 24-well Matrigel-coated invasion chambers over an incubation period of 15h.

Hydroxyproline assay

Hydroxyproline contents of whole mouse lung tissues were determined according to a previously described method 21 days after initiation of BLM-induced lung injury (Shetty et al., 2017). Lung homogenates were hydrolyzed in 6N HCl at 120 °C for 24h. Hydrolysates were mixed with an equal volume of citrate/acetate buffer (pH 6.0) and 100 μL chloramine-T solution in a 96-well plate. The mixtures were incubated for 20 minutes at room temperature; then, 100 μL Ehrlich's solution was added, and incubation was continued at 45°C for 1h. Absorbance at 550 nm was measured, and hydroxyproline content in each lung tissue homogenate was determined from a standard curve.

QUANTIFICATION AND STATISTICAL ANALYSIS

Difference between two groups were analyzed by Student's *t* test. Multiple groups were analyzed by one-way analysis of variance (ANOVA with Tukey's multiple comparisons) tests. Prism 9.0 (GraphPad) was used for graph editing and the statistical analyses.